

NEUROSCIENCE

An endogenous GLP-1 circuit engages VTA GABA neurons to regulate mesolimbic dopamine neurons and attenuate cocaine seeking

Riley Merkel^{1,2}, Nicole S. Hernandez^{1,2}, Vanessa Weir^{1,2,3}, Yafang Zhang^{1,2}, Antonia Caffrey^{1,2}, Matthew T. Rich⁴, Richard C. Crist², Benjamin C. Reiner², Heath D. Schmidt^{1,2*}

Recent studies show that systemic administration of a glucagon-like peptide-1 receptor (GLP-1R) agonist is sufficient to attenuate cocaine seeking. However, the neural mechanisms mediating these effects and the role of endogenous central GLP-1 signaling in cocaine seeking remain unknown. Here, we show that voluntary cocaine taking decreased plasma GLP-1 levels in rats and that chemogenetic activation of GLP-1-producing neurons in the nucleus tractus solitarius that project to the ventral tegmental area (VTA) decreased cocaine seeking. Single-nuclei transcriptomics and FISH studies revealed that GLP-1Rs are expressed primarily on GABA neurons in the VTA. Using in vivo fiber photometry, we found that the efficacy of a systemic GLP-1R agonist to attenuate cocaine seeking was associated with increased activity of VTA GABA neurons and decreased activity of VTA dopamine neurons. Together, these findings suggest that targeting central GLP-1 circuits may be an effective strategy toward reducing cocaine relapse and highlight a functional role of GABAergic GLP-1R-expressing midbrain neurons in drug seeking.

INTRODUCTION

Cocaine use disorder (CUD) remains a critical public health concern in the United States. Unfortunately, the prevalence of cocaine use, as well as the incidence of fatal overdoses involving cocaine, has increased year-over-year (1, 2). Despite decades of focused preclinical and clinical studies that have advanced our understanding of the anatomical, neurochemical, molecular, and epigenetic bases of psychostimulant addiction, a safe and efficacious pharmacotherapy for CUD remains to be discovered (3). Thus, an improved understanding of the neurobiological mechanisms that regulate cocaine taking and seeking is needed to inform conceptually new approaches to treating CUD.

An emerging literature indicates that activation of central glucagon-like peptide-1 receptors (GLP-1Rs) reduces the rewarding and reinforcing effects of addictive drugs (4–7). GLP-1Rs are primarily coupled to Gs, and their activation leads to increased cyclic adenosine 3',5'-monophosphate (cAMP) signaling (although GLP-1Rs have been shown to engage other intracellular signaling cascades as well) (8). Previously, we identified a systemic dose of the GLP-1R agonist exen-4 that selectively attenuated the reinstatement of cocaine-seeking behavior in rats (9), an animal model of drug relapse. These effects were mediated, in part, by activation of GLP-1Rs in the ventral tegmental area (VTA) (9). Consistent with these effects, direct activation of GLP-1Rs in the VTA is sufficient to attenuate cocaine seeking (9). In addition to expressing GLP-1Rs (10, 11), the VTA also receives direct monosynaptic projections from GLP-1-producing preproglucagon (PPG) neurons in the nucleus tractus solitarius (NTS) (12, 13).

Together with our behavioral pharmacology studies, this anatomy suggests that activating endogenous GLP-1-producing NTS→VTA projections may suppress cocaine-seeking behaviors during abstinence. However, no studies, to date, have targeted endogenous GLP-1-producing NTS circuits to reduce the reinstatement of drug-seeking behavior during abstinence.

The mechanisms by which GLP-1R activation in the midbrain attenuates cocaine seeking remain unknown. Therefore, phenotyping GLP-1R-expressing cells in the VTA and determining how GLP-1R activation alters the activity of these neurons during cocaine seeking are essential “next steps” toward developing the next-generation of GLP-1R-based therapies to treat CUD. In the present study, we (i) assessed the functional role of endogenous VTA GLP-1 signaling in cocaine seeking using projection-specific chemogenetic approaches, (ii) determined cell type-specific expression patterns of GLP-1Rs in the VTA using fluorescence in situ hybridization (FISH) and single-nuclei RNA sequencing (snRNA-seq) methods, and (iii) used in vivo fiber photometry in freely moving transgenic rats to further our understanding of the cell type-specific mechanisms in the midbrain underlying the suppressive effects of a GLP-1R agonist on cocaine seeking. Our findings indicate that voluntary cocaine taking decreased circulating GLP-1 levels and that chemogenetic activation of NTS→VTA projections was sufficient to attenuate cocaine seeking via increased GLP-1 signaling in the VTA. Using FISH and snRNA-seq, we phenotyped GLP-1R-expressing cells in the midbrain and discovered that GLP-1Rs are expressed primarily on γ -aminobutyric acid (GABA) neurons in the VTA. Lastly, using in vivo calcium imaging, we showed that the efficacy of systemic exen-4 is associated with dynamic changes in activity of VTA GABA and dopamine neurons that are associated with decreased cocaine seeking. Together, these findings reveal a functionally relevant cell type-specific mechanism underlying the suppressive effects of GLP-1R agonists on cocaine seeking and highlight an endogenous GLP-1-expressing circuit that could be targeted to treat CUD and reduce cocaine relapse.

Copyright © 2025 The Authors, some rights reserved; exclusive licensee American Association for the Advancement of Science. No claim to original U.S. Government Works. Distributed under a Creative Commons Attribution License 4.0 (CC BY).

¹Department of Biobehavioral Health Sciences, School of Nursing, University of Pennsylvania, Philadelphia, PA 19104, USA. ²Department of Psychiatry, Perelman School of Medicine, University of Pennsylvania, Philadelphia, PA 19104, USA. ³Vaegelos College of Physicians and Surgeons, Columbia University, New York, NY 10032, USA. ⁴Department of Psychiatry, Brain Health Institute, Robert Wood Johnson Medical School, Rutgers University, Piscataway, NJ 08854, USA.

*Corresponding author. Email: hschmidt@nursing.upenn.edu

RESULTS

Voluntary cocaine taking decreases plasma GLP-1 levels

To determine whether voluntary cocaine taking and subsequent abstinence alter plasma GLP-1 levels, blood samples were drawn from cocaine-experienced rats and their corresponding yoked saline controls at three time points (Fig. 1A). Plasma GLP-1 concentrations (picograms per milliliter) were significantly decreased in cocaine-experienced rats versus yoked saline controls following 21 days of self-administration (Fig. 1B) and 1 day of extinction (Fig. 1C). In contrast, there were no significant differences in plasma GLP-1 levels between cocaine-experienced rats and yoked saline controls following 7 days of extinction (Fig. 1D). Behavioral data corresponding to blood collection timepoints are presented in fig. S1. These findings, together with our previous studies showing that systemic and intracranial infusions of a GLP-1R agonist attenuated cocaine reinstatement (9, 14, 15), support the hypothesis that decreased endogenous GLP-1 signaling facilitates/promotes cocaine-taking and cocaine-seeking behaviors (5).

Activation of NTS neurons that project to the VTA selectively attenuates drug seeking in cocaine-experienced rats

Despite growing evidence that GLP-1R agonist pharmacotherapy is sufficient to reduce cocaine seeking (9, 14), no studies have investigated the role of endogenous GLP-1-producing neural circuits in drug-seeking behavior. To selectively activate endogenous GLP-1-producing NTS neurons that project to the VTA, the retrogradely infecting virus canine adenovirus-2-expressing Cre recombinase (CAV2-Cre) was infused into the VTA, and a Cre-dependent virus expressing a neural activating DREADD [AAV-DIO-hM3D(Gq)-mCherry] was infused into the NTS (Fig. 2, A and B). Immunohistochemistry (IHC) was performed on NTS sections to label c-Fos after clozapine *N*-oxide (CNO) injection in both hM3D(Gq)-expressing rats and mCherry control rats (Fig. 2C). CNO significantly increased

c-Fos expression in ~55% of NTS hM3D(Gq)-expressing neurons compared to <5% of mCherry-expressing neurons (Fig. 2D). Whole-cell current clamp recordings were conducted to further validate the ability of CNO to increase activity of hM3D(Gq)-expressing NTS neurons compared to mCherry-expressing control neurons. CNO increased NTS cell firing in hM3D(Gq)-expressing rats (Fig. 2E) and had no effect on NTS cell firing in mCherry control rats (Fig. 2F).

To determine the functional role of NTS→VTA projections in cocaine seeking, rats were pretreated with vehicle or CNO [0.1 or 1.0 mg/kg, intraperitoneally (ip)] before a cocaine priming-induced reinstatement test session. CNO dose-dependently attenuated cocaine seeking in hM3D(Gq)-expressing rats (Fig. 2G). A previous study showed that activation of GLP-1-producing NTS neurons that project to the VTA transiently reduced food intake in drug-naïve mice (16). In addition, GLP-1R agonists are known to decrease food intake and produce nausea/emesis in both drug-naïve rodents and humans (4, 17–19). We screened for these potential adverse effects in our cocaine-experienced rats and found no effects of CNO on cumulative chow intake (Fig. 2H) and 24-hour body weight gain (Fig. 2I) on reinstatement test days. Together, these studies indicate that activation of NTS→VTA projections is sufficient to reduce cocaine seeking during abstinence and that drug seeking is more sensitive to central GLP-1 modulation than nondrug motivated behaviors in cocaine-experienced rats.

Although CNO is often used as the inert ligand for DREADDs, studies show minimal, yet notable, reverse metabolism to clozapine, an active metabolite which could bind to non-DREADD receptors and produce off-target effects on behavior (20). To control for this, a separate group of rats was infused with the control virus AAV-DIO-mCherry into the NTS and allowed to self-administer cocaine. In contrast to the effects seen in hM3D(Gq)-expressing rats, CNO had no effect on cocaine seeking in rats infused with the mCherry

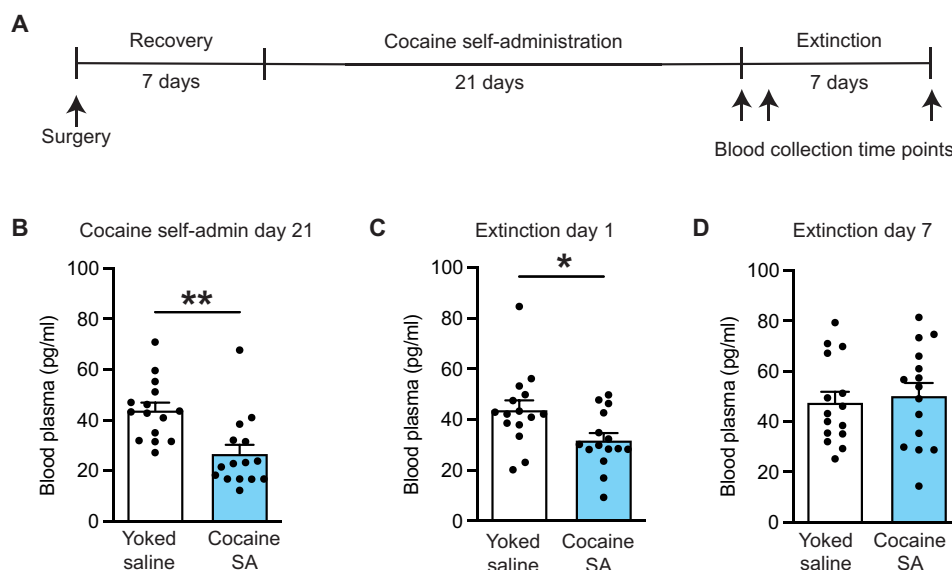


Fig. 1. Cocaine self-administration decreases circulating GLP-1 levels. (A) Schematic illustrating the experimental timeline and blood collection time points [yoked saline: $n = 15$ (6 female and 9 male rats); cocaine self-administration: $n = 15$ (6 female and 9 male rats)]. (B and C) Plasma GLP-1 concentrations were significantly decreased in cocaine-experienced rats following 21 days of cocaine self-administration (unpaired t test: $t_{28} = 3.604$, $**P = 0.0012$) and 1 day of extinction (unpaired t test: $t_{28} = 2.474$, $*P = 0.0197$). (D) There were no significant differences in plasma GLP-1 levels between cocaine-experienced rats and yoked saline controls following 7 days of extinction (unpaired t test: $t_{28} = 0.4042$, $P = 0.6891$). Data are mean \pm SEM. SA, self-administration.

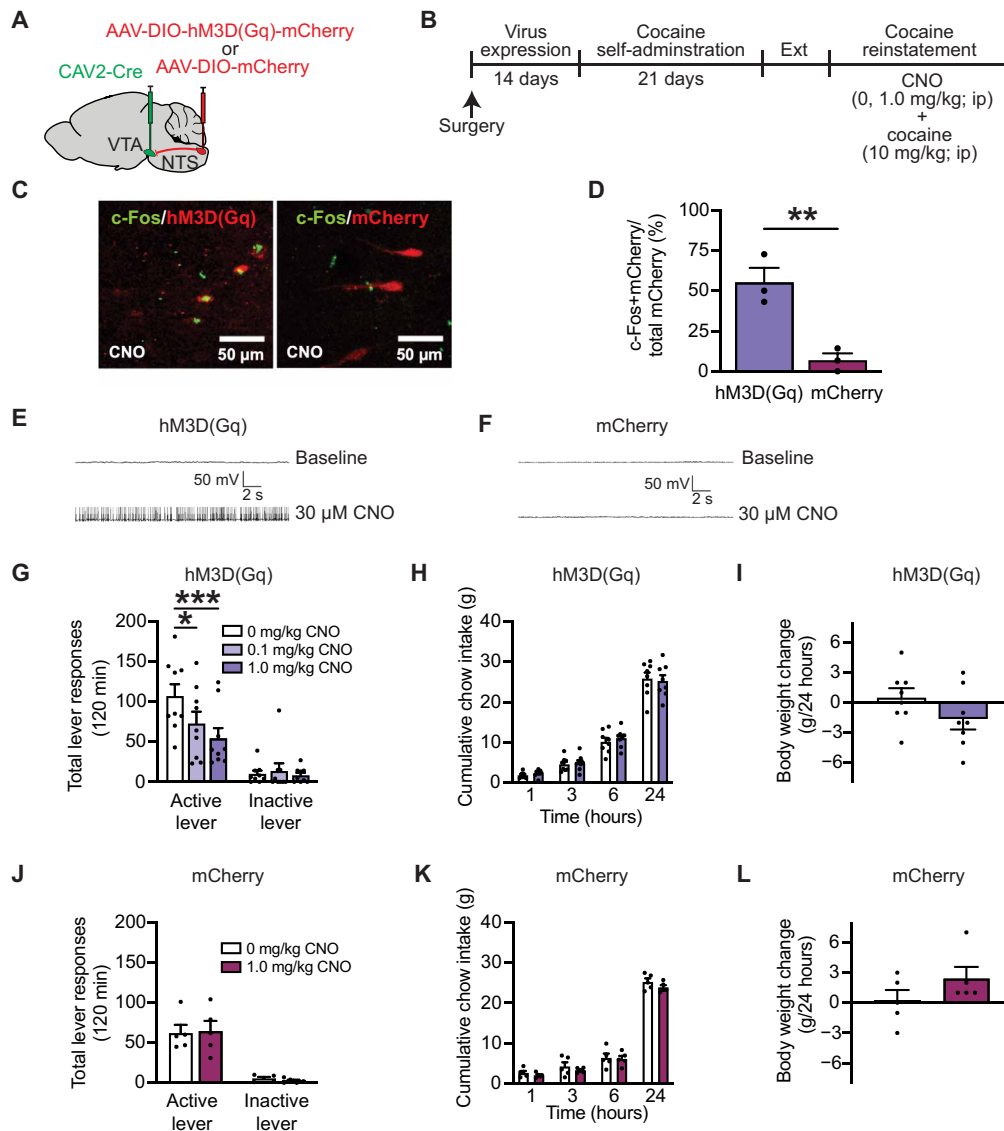


Fig. 2. Activating NTS→VTA projections attenuates cocaine seeking. (A and B) Illustration of viral approach and experimental timeline. (C) Representative images showing increased c-Fos expression in hM3D(Gq)-expressing NTS neurons of rats treated with CNO versus mCherry controls. (D) CNO significantly increased c-Fos expression in ~55% of hM3D(Gq)-expressing NTS neurons versus <5% of mCherry-expressing NTS neurons ($n = 3$ per treatment; unpaired t test: $t_4 = 4.911$, $**P = 0.0080$). (E and F) Representative whole-cell current-clamp traces showing increased firing of hM3D(Gq)-expressing NTS neurons and no change in firing of mCherry-expressing NTS neurons following CNO administration. (G) CNO dose-dependently decreased active lever presses in rats expressing hM3D(Gq) in NTS neurons that project to the VTA [$n = 9$ (three female and six male rats); two-way RM analysis of variance (ANOVA), treatment \times lever interaction: $F_{2,16} = 5.362$, $P = 0.0165$; Bonferroni's test: vehicle versus CNO (0.1 mg/kg), $*P = 0.025$; vehicle versus CNO (1.0 mg/kg), $***P = 0.0009$]. (H and I) CNO did not reduce cumulative chow intake (two-way RM ANOVA, treatment: time \times treatment: $F_{3,21} = 0.6343$, $P = 0.6012$) or 24-hour body weight gain (paired t test: $t_7 = 1.838$, $P = 0.1087$) in rats expressing hM3D(Gq) in NTS neurons that project to the VTA [$n = 8$ (three female and five male rats)]. (J to L) CNO had no effects on cocaine seeking (two-way RM ANOVA, treatment \times lever: $F_{1,4} = 0.6170$, $P = 0.4761$), cumulative chow intake (two-way RM ANOVA, treatment \times lever: $F_{3,12} = 0.421$, $P = 0.7419$), or 24-hour body weight gain (paired t test: $t_4 = 2.400$, $P = 0.0743$) in mCherry-expressing control rats [$n = 5$ (three female and two male rats)]. Data are mean \pm SEM.

control virus (Fig. 2J). These findings indicate that CNO itself does not suppress drug-seeking behavior during abstinence following cocaine self-administration. Moreover, there were no effects of CNO on cumulative chow intake (Fig. 2K) and 24-hour body weight gain (Fig. 2L) in mCherry control rats. Thus, the suppressive effects of activating NTS→VTA projections on cocaine seeking are not due to off-target effects of CNO or a CNO metabolite.

Activation of NTS→VTA projections attenuates cocaine seeking via a GLP-1-dependent mechanism of action in the VTA

The NTS consists of a heterogeneous population of neurons that could mediate the behavioral effects shown in Fig. 2. Therefore, our next goal was to determine whether the suppressive effects of activating NTS→VTA projections on cocaine seeking were due to increased

GLP-1 signaling in the VTA. Rats were infused with CAV2-Cre into the VTA and AAV-DIO-hM3D(Gq)-mCherry into the NTS and implanted with guide cannula aimed at the VTA (Fig. 3A). Rats then underwent cocaine self-administration, extinction, and reinstatement (Fig. 3B). IHC analyses revealed hM3D(Gq) colocalized with GLP-1 in NTS neurons that project to the VTA (Fig. 3C). Before reinstatement test sessions, the GLP-1R antagonist exendin-(9-39) (10 μ g/100 nl) was infused directly into the VTA 10 min before administration of CNO (1.0 mg/kg, ip) to determine whether pharmacological inhibition of VTA GLP-1Rs is sufficient to block the suppressive effects of chemogenetic activation of NTS→VTA projections on cocaine seeking (Fig. 3D). Intra-VTA exendin-(9-39) pretreatment blocked the ability of CNO to attenuate cocaine seeking (Fig. 3, E and F), indicating that the suppressive effects of activating endogenous NTS→VTA circuits on drug seeking depend, in part, on enhanced GLP-1 signaling in the midbrain.

GLP-1Rs are expressed primarily on GABAergic cells in the VTA

Next, we showed that a behaviorally relevant dose of exendin-4 that reduced cocaine seeking (9, 14) crossed the blood-brain barrier, bound putative GLP-1Rs on neurons in the VTA, and induced c-Fos

expression in these neurons (fig. S2). The exact cell types expressing GLP-1Rs in the VTA, however, remain unclear. To further investigate the mechanisms by which GLP-1R agonist pharmacotherapy alters midbrain neuron activity and attenuates cocaine seeking, we used FISH to phenotype GLP-1R-expressing cells in the VTA. We found that ~90% of *Glp1r*-expressing cells coexpress *Gad1* and that no *Glp1r* transcripts were detected in *Th*-positive cells (Fig. 4, A and B). In addition, ~10% of *Glp1r*-expressing cells belonged to nonidentified cell type(s) (Fig. 4B). When quantifying expression throughout the rostral-caudal axis of the VTA, FISH analyses revealed a greater number *Glp1r*-expressing, *Gad1*-positive cells in the posterior VTA when compared to more anterior subregions of the VTA (Fig. 4, C and D). To validate the expression pattern of *Glp1r*, we performed snRNA-seq on rat VTA samples. Neurons and all major glial populations were identified in the snRNA-seq dataset (Fig. 4, E and F). Consistent with our FISH results, the majority of *Glp1r*-expressing nuclei also expressed *Gad1*, and there was no observed overlap between *Glp1r* and *Th* expression (Fig. 4G). These anatomical studies clearly showed that GLP-1Rs are expressed primarily on GABA neurons in the VTA and support the hypothesis that GLP-1R agonists increase inhibitory GABA transmission in the VTA to reduce cocaine seeking.

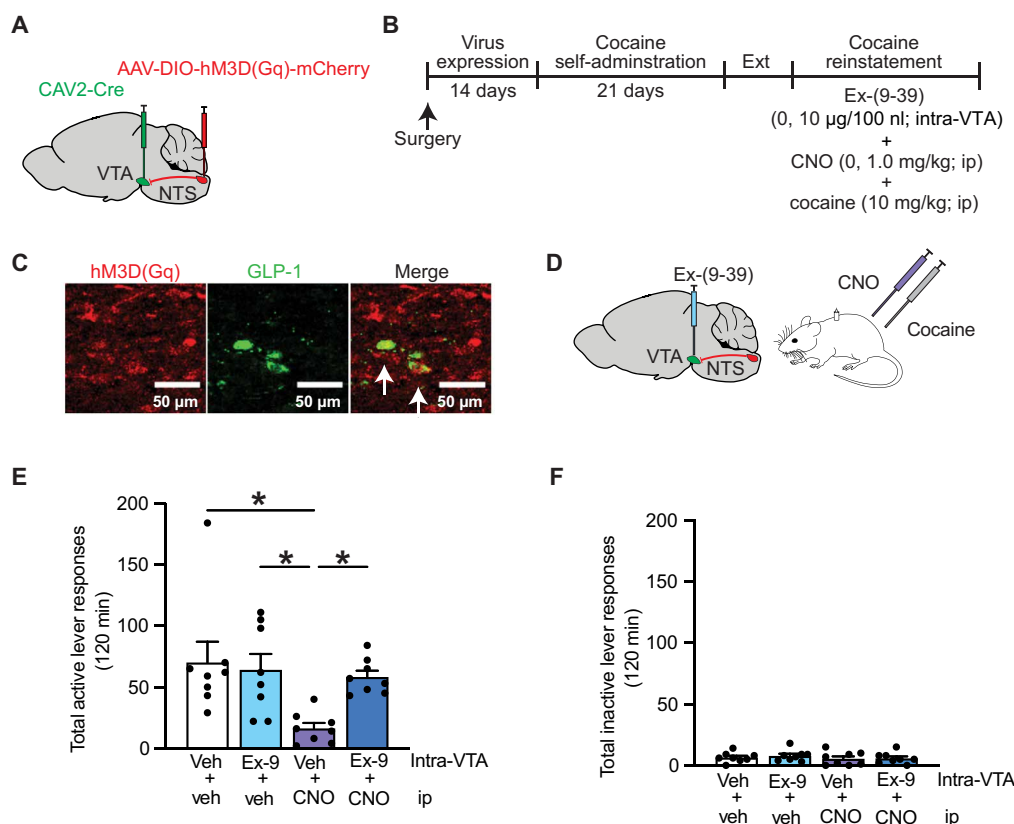


Fig. 3. Pharmacological inhibition of VTA GLP-1Rs blocks the suppressive effects of activating NTS→VTA projections on cocaine seeking. (A and B) Illustration of viral approach and experimental timeline wherein CAV2-Cre and a Cre-dependent AAV-expressing hM3D(Gq) were infused into the VTA and NTS, respectively, before the cocaine self-administration phase of the experiment. (C) Representative images of hM3D(Gq)-expressing NTS neurons that coexpress GLP-1. (D) Schematic depicting reinstatement test session treatment conditions. Exendin-(9-39) was infused into the VTA before activating endogenous NTS→VTA projections with CNO. (E) Intra-VTA exendin-(9-39) (Ex-9) prevented the ability of CNO to suppress active lever presses during reinstatement test sessions ($n = 8$ (three female and five male rats); two-way RM ANOVA, systemic treatment \times intra-VTA treatment: $F_{1,7} = 8.775$, $P = 0.0210$; Bonferroni's test: vehicle (veh)/vehicle versus vehicle/CNO, $*P = 0.0132$; vehicle/CNO versus Ex-(9-39)/vehicle, $*P = 0.0249$; vehicle/CNO versus Ex-(9-39)/CNO, $*P = 0.0441$). (F) Intra-VTA exendin-(9-39) had no effect on inactive lever responses ($n = 8$; two-way RM ANOVA, systemic treatment: $F_{1,7} = 2.333$, $P = 0.1705$; intra-VTA treatment: $F_{1,7} = 0.320$, $P = 0.5891$; systemic treatment \times intra-VTA treatment: $F_{1,7} = 0.138$, $P = 0.7207$). Data are mean \pm SEM.

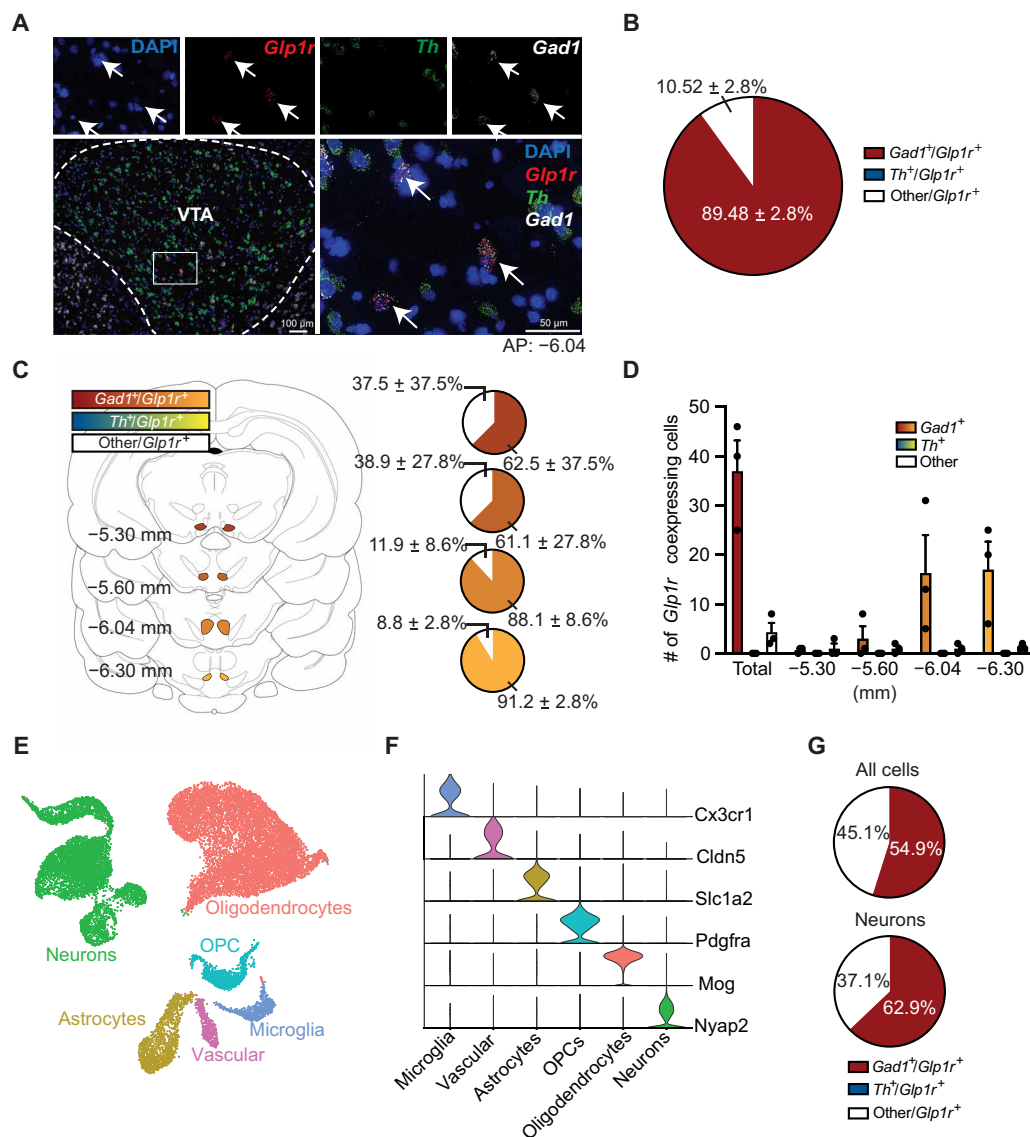


Fig. 4. GLP-1Rs are expressed primarily on GABAergic neurons in the VTA. (A) FISH revealed *Glp1r* transcripts coexpressed with *Gad1* transcripts in the VTA [4',6-diamidino-2-phenylindole (DAPI; blue), *Glp1r* (red), *Th* (green), and *Gad1* (white)]. (B) About 90% of all *Glp1r*-expressing neurons in the VTA coexpress *Gad1*. No *Glp1r* transcripts were detected in *Th*-positive cells ($n = 3$ rats; four slices per rat). (C and D) Both the total percentage and number of *Glp1r*-positive cells coexpressing *Gad1* are greater in posterior regions of the VTA ($n = 3$ rats). (E) Uniform manifold approximation and projection dimension reduction plot for snRNA-seq from the VTA of drug-naïve rats ($n = 5$). Nuclei are colored by major cell type. (F) Violin plot showing normalized expression of marker genes for major VTA cell types. (G) Pie charts displaying the percentage of *Glp1r*-expressing cells (top) or neurons (bottom) that coexpress *Gad1*, *Th*, or neither marker in the snRNA-seq dataset. Data are mean ± SEM.

Systemic GLP-1R agonist pharmacotherapy increases activity of VTA GABA neurons and attenuates cocaine seeking

Our FISH and snRNA-seq studies revealed that GLP-1Rs expressed primarily on GABA neurons in the VTA (Fig. 4). However, it is unclear how GLP-1R activation influences the activity of VTA GABA neurons in cocaine-experienced rats and how these cell type-specific cellular responses are related to cocaine-seeking behavior. We used in vivo fiber photometry in transgenic rats to determine how GLP-1R agonist pharmacotherapy alters activity of VTA GABA neurons during reinstatement test sessions. To measure changes in intracellular calcium levels in midbrain GABA neurons during cocaine

seeking, a Cre-dependent GCaMP8f virus was infused into the VTA of rats expressing Cre-recombinase under the *GAD* promoter, and a fiberoptic cannula was implanted directly above the infusion site (Fig. 5A). A representative image of subregion-specific viral expression is shown in Fig. 5B. Fluorescent labeling of *eGfp*, *Th*, and *Gad1* mRNA transcripts using FISH confirmed selective GCaMP8f expression in *Gad1*-positive neurons in the VTA (Fig. 5B).

To determine whether GLP-1R activation increases calcium dynamics in VTA GABA neurons during cocaine seeking, rats were pretreated with vehicle or exendin-4 (2.0 μg/kg, ip) before a cocaine priming-induced reinstatement test session. Consistent with our prior studies (9, 14), exendin-4 significantly reduced cocaine seeking

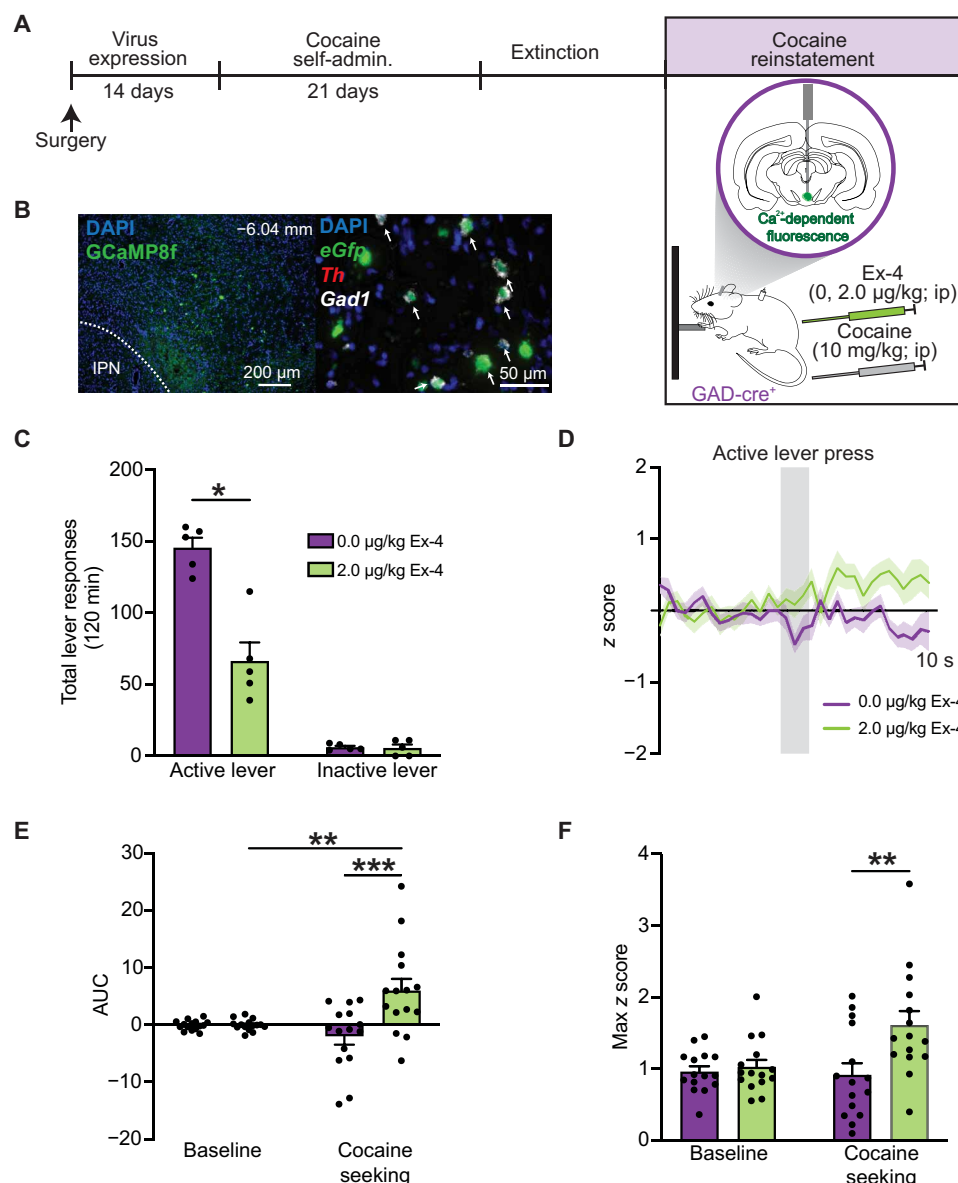


Fig. 5. Systemic GLP-1R agonist pharmacotherapy increases VTA GABA neuron activity and decreases cocaine seeking. (A) Schematic illustrating the viral approach and experimental timeline wherein a Cre-dependent AAV-expressing GCaMP8f virus was infused into the VTA of GAD-Cre rats to measure intracellular calcium dynamics in VTA GABA neurons during reinstatement test sessions. (B) Representative image of GCaMP8f viral expression in the VTA. FISH confirmed selective GCaMP8f expression in *Gad1*-positive cells [DAPI (blue), *eGfp* (green), *Th* (red), and *Gad1* (white)]. IPN, Interpeduncular nucleus. (C) Systemic exendin-4 administration decreased active lever responses during cocaine reinstatement test sessions [$n = 5$ (three female and two male rats); two-way RM ANOVA, treatment \times lever: $F_{1,4} = 19.64$, $P = 0.0114$; Bonferroni's test: vehicle versus exendin-4, * $P = 0.0129$]. (D) Normalized z score traces during cocaine seeking in rats pretreated with vehicle or exendin-4 ($n = 5$ rats; three active lever presses per rat per treatment). (E) Cocaine seeking significantly increased the AUC of recorded Ca^{2+} signals from VTA GABA neurons in rats treated with exendin-4, but not vehicle ($n = 15$; two-way RM ANOVA, treatment \times time: $F_{1,28} = 9.652$, $P = 0.0043$; Bonferroni's test: baseline versus cocaine seeking in rats treated with exendin-4, ** $P = 0.0099$). The AUC from rats treated with exendin-4 was also significantly increased during cocaine seeking compared to vehicle-treated controls (Bonferroni's test: 0.0 versus 2.0 $\mu\text{g/kg}$ exendin-4 during cocaine seeking, *** $P = 0.0001$). (F) Exendin-4 significantly increased maximum z scores in VTA GABA neurons during cocaine seeking compared to vehicle-treated controls ($n = 15$; two-way RM ANOVA, treatment \times time: $F_{1,28} = 4.110$, $P = 0.0522$; Bonferroni's test: 0.0 versus 2.0 $\mu\text{g/kg}$ exendin-4 during cocaine seeking, ** $P = 0.0036$). Data are mean \pm SEM.

in GAD-Cre rats (Fig. 5C). Cell type-specific normalized z score traces during cocaine seeking are presented in Fig. 5D. Area under the curve (AUC) and maximum z scores were calculated from these traces. AUC was significantly increased during cocaine seeking compared to baseline in VTA GABA neurons of rats pretreated with exendin-4, indicating that cocaine-seeking behavior evokes transient

increases in VTA GABA neuron activity in exendin-4-treated rats (Fig. 5, E and F). AUC and maximum z scores were significantly increased in VTA GABA neurons from exendin-4-treated rats compared to VTA GABA neurons from vehicle-treated controls (Fig. 5, E and F). These results indicate that exendin-4 pretreatment produces greater activity of VTA GABA neurons during drug seeking

compared to vehicle-treated controls. Normalized z score traces associated with inactive lever presses during reinstatement test sessions are presented in fig. S3A. There were no effects of treatment on AUC and maximum z scores from VTA GABA neurons following inactive lever responses during reinstatement test sessions (fig. S3, B and C). To confirm that these calcium dynamics were specific to cocaine-seeking behavior, a separate group of GAD-Cre rats was allowed to self-administer saline before undergoing extinction and subsequent reinstatement tests. There were no effects of vehicle or exendin-4 on AUC or maximum z scores from VTA GABA neurons following active lever presses during the reinstatement test sessions in drug-naïve rats (fig. S4, A to D). Together, these findings indicate that GLP-1R agonist pharmacotherapy increases calcium dynamics in VTA GABA neurons during cocaine seeking, effects associated with decreased drug-seeking behavior during abstinence.

To confirm that activation of GABAergic neurons in the VTA is sufficient to attenuate cocaine seeking, AAV-DIO-hM3D(Gq)-mCherry was infused into the VTA of rats expressing Cre-recombinase under the *GAD* promoter (fig. S5). Rats were then allowed to self-administer cocaine for 21 days before extinction and subsequent reinstatement test sessions. Rats were pretreated with vehicle or CNO (0.1 or 1.0 mg/kg, ip) before a cocaine priming-induced reinstatement test session. CNO dose-dependently decreased cocaine seeking, effects associated with increased activation of GABAergic neurons in the VTA (fig. S5). These findings support our hypothesis that the suppressive effects of exendin-4 on cocaine seeking are due, in part, to activating inhibitory GABA circuits in the midbrain.

Systemic GLP-1R agonist pharmacotherapy reduces activity of VTA dopamine neurons and attenuates cocaine seeking

Systemic GLP-1R agonist administration reduced cocaine-evoked dopamine release in the nucleus accumbens (NAc) (21), a downstream target of VTA dopamine neurons known to play a critical role in cocaine seeking (22, 23). Given that GLP-1R agonist pharmacotherapy increased activity of VTA GABA neurons in cocaine-experienced rats (Fig. 5), we hypothesized that this cell type-specific response would coincide with decreased VTA dopamine cell activity and represent one mechanism by which systemic exendin-4 suppresses cocaine-seeking behavior. We used in vivo fiber photometry in transgenic rats to determine how GLP-1R agonist pharmacotherapy alters activity of VTA dopamine neurons during cocaine reinstatement test sessions. To measure changes in intracellular calcium levels in midbrain dopamine neurons during cocaine seeking, a Cre-dependent GCaMP8f virus was infused into the VTA of rats expressing Cre-recombinase under the *Th* promoter, and a fiberoptic cannula was implanted directly above the infusion site (Fig. 6A). A representative image of subregion-specific viral spread is shown in Fig. 6B. Fluorescent labeling of *eGFP*, *Th*, and *Gad1* mRNA transcripts using FISH confirmed selective GCaMP8f expression in *Th*-positive neurons in the VTA (Fig. 6B).

To determine whether GLP-1R activation suppresses calcium dynamics in VTA dopamine neurons during cocaine seeking, rats were pretreated with vehicle or exendin-4 (2.0 μ g/kg, ip) before a cocaine priming-induced reinstatement test session (Fig. 6A). Consistent with our prior studies (9, 14) and the reinstatement studies above in GAD-Cre rats (Fig. 5C), exendin-4 significantly reduced cocaine seeking in TH-Cre rats (Fig. 6C). Cell type-specific normalized z score traces during cocaine seeking are presented in Fig. 6D. AUC and maximum z scores were significantly increased during cocaine seeking compared to baseline in VTA dopamine

neurons of vehicle-treated rats. These findings indicate that cocaine-seeking behavior evokes transient increases in VTA dopamine neuron activity (Fig. 6, E and F). Pretreatment with exendin-4 blocked cocaine seeking-evoked increases in AUC and maximum z scores (Fig. 6, E and F). Normalized z score traces associated with inactive lever presses during reinstatement tests are presented in fig. S6A. No effects of treatment were found on AUC and maximum z scores from VTA dopamine neurons following inactive lever responses during the reinstatement test sessions (fig. S6, B and C). To confirm that these calcium dynamics were specific to cocaine-seeking behavior, a separate group of TH-Cre rats was allowed to self-administer saline before undergoing extinction and subsequent reinstatement test sessions. There were no effects of vehicle or exendin-4 on AUC or maximum z scores from VTA dopamine neurons following an active lever press in drug-naïve rats (fig. S7). Together, these findings indicate that activity of VTA dopamine neurons is significantly increased during cocaine seeking and that GLP-1R agonist pharmacotherapy prevents/blocks this cellular response and suppresses drug-seeking during abstinence.

DISCUSSION

An emerging literature indicates that activating central GLP-1Rs is sufficient to reduce cocaine-seeking behavior (9, 14, 15), findings that support translational studies focused on repurposing GLP-1R agonists to treat CUD (5, 24). However, the neural mechanisms underlying the efficacy of GLP-1R agonists to reduce cocaine seeking and the role of central GLP-1-producing neural circuits in cocaine seeking are unknown. Here, we discovered that cocaine self-administration and acute withdrawal decreased plasma GLP-1 levels and that chemogenetic activation of GLP-1-producing NTS neurons that project to the VTA is sufficient to attenuate cocaine seeking during abstinence. We also showed that GLP-1Rs are expressed primarily on GABA neurons in the VTA and that the suppressive effects of a GLP-1R agonist on cocaine seeking are associated with increased activity of VTA GABA neurons and decreased activity of VTA dopamine neurons. These cell type-specific cellular responses expand our understanding of the neural mechanisms underlying the efficacy of GLP-1R agonists on cocaine seeking. Our findings suggest that targeting endogenous GLP-1-producing neural circuits may reduce cocaine craving-induced relapse and further support the potential for GLP-1R-based pharmacotherapeutic approaches to treat CUD.

Endogenous GLP-1 signaling is dynamically altered by cocaine taking and abstinence

A pilot study of human cocaine users showed that intravenous cocaine self-administration decreased serum GLP-1 levels, effects associated with cocaine-related cardiorespiratory and subjective responses (25). While it is not clear how decreased serum GLP-1 may promote the subjective experiences of cocaine in humans, these results suggest that reduced GLP-1 signaling may drive ongoing cocaine taking. We extended these findings to a preclinical model of CUD and found that plasma GLP-1 concentrations were significantly decreased following intravenous cocaine self-administration and acute abstinence in rats. Given that systemic administration of GLP-1R agonists reduce cocaine taking (26) and seeking (9, 14) in rodents, these results suggest that decreased endogenous GLP-1 signaling may facilitate cocaine-seeking behavior. Consistent with these results, expression of PPG mRNA, a necessary precursor of GLP-1 production, is decreased

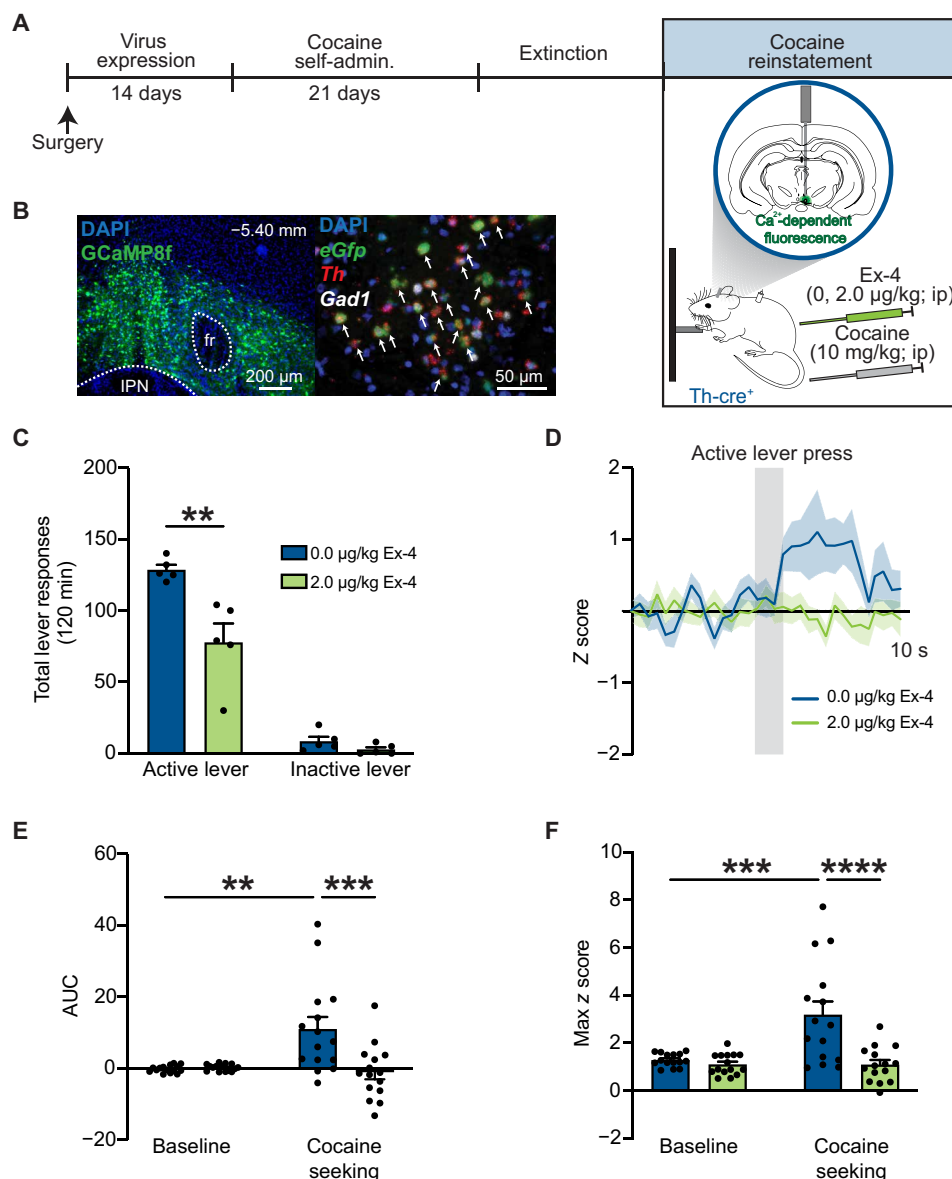


Fig. 6. Systemic GLP-1R agonist pharmacotherapy attenuates VTA dopamine neuron activity and decreases cocaine seeking. (A) Schematic illustrating viral approach and experiment timeline where a Cre-dependent AAV-expressing GCaMP8f virus was infused into the VTA of TH-Cre rats to measure intracellular calcium dynamics in VTA dopamine neurons during reinstatement tests sessions. (B) Representative image of GCaMP8f viral expression in the VTA. FISH confirmed selective GCaMP8f expression in *Th*-positive cells [DAPI (blue), *eGfp* (green), *Th* (red), and *Gad1* (white)]. (C) Systemic extendin-4 administration decreased active lever responses during cocaine reinstatement test sessions [$n = 5$ (two female and three male rats); two-way RM ANOVA, treatment \times lever: $F_{1,4} = 39.66$, $P = 0.0032$; Bonferroni's test: vehicle versus extendin-4: $**P = 0.0023$]. (D) Normalized z score traces during cocaine seeking in rats pretreated with vehicle or extendin-4 ($n = 5$ rats; three active lever presses per rat per treatment). (E) Cocaine seeking significantly increased the AUC of recorded Ca^{2+} signals from VTA dopamine neurons in rats treated with vehicle (two-way RM ANOVA, treatment \times time: $F_{1,28} = 10.71$, $P = 0.0028$; Bonferroni's test: baseline versus cocaine seeking in vehicle-treated controls: $**P = 0.0011$). Extendin-4 pretreatment significantly attenuated cocaine seeking-evoked increases in VTA dopamine neuron activity (Bonferroni's test: 0.0 versus 2.0 $\mu\text{g/kg}$ extendin-4 during cocaine seeking: $***P = 0.0002$). (F) Cocaine seeking significantly increased maximum z scores in VTA dopamine neurons in rats treated with vehicle (two-way RM ANOVA, treatment \times time: $F_{1,28} = 11.37$, $P = 0.0022$; Bonferroni's test: baseline versus cocaine seeking in vehicle-treated controls: $***P = 0.0002$). Extendin-4 pretreatment significantly decreased maximum z scores in VTA dopamine neurons during cocaine seeking compared to vehicle [Bonferroni's test: cocaine seeking (0.0 $\mu\text{g/kg}$) versus cocaine seeking (2.0 $\mu\text{g/kg}$), $****P < 0.0001$]. Data are mean \pm SEM.

in the NTS following 7 days of cocaine abstinence, a time point associated with robust cocaine-seeking behavior in rats (9). Together, these findings support the hypothesis that decreased endogenous GLP-1 signaling promotes/facilitates drug seeking and that activating central GLP-1-producing neural circuits may attenuate cocaine-seeking behavior during abstinence.

While plasma GLP-1 levels are significantly decreased following cocaine self-administration, our prior studies suggest a trend toward increased NTS PPG mRNA expression at the same time point (9). These findings indicate that cocaine taking and subsequent abstinence have differential effects on peripheral versus central GLP-1 expression. Therefore, it is also possible that reduced peripheral GLP-1

expression contributes to the subjective effects of cocaine and promotes drug taking, while increased central GLP-1 signaling functions as a compensatory response to reduce ongoing drug taking (25). Disentangling the roles of peripheral and central GLP-1 signaling in cocaine-mediated behaviors is an important future direction of the lab.

Targeted activation of endogenous GLP-1-producing “anticraving” circuits attenuates cocaine seeking

The VTA receives monosynaptic projections from GLP-1-producing neurons in the NTS (27) and plays a critical role in the reinstatement of cocaine-seeking behavior (4). While cocaine taking does not alter GLP-1R expression in the VTA, abstinence following cocaine self-administration decreased PPG mRNA expression in the NTS (9). These results suggest that decreased PPG expression in the NTS may facilitate/promote cocaine seeking via reduced GLP-1 tone in target nuclei, including the VTA (5). Here, we showed that chemogenetic activation of GLP-1-producing NTS neurons that project to the VTA is sufficient to suppress drug seeking in cocaine-experienced rats. These findings establish a functional role for GLP-1-producing NTS→VTA projections in cocaine seeking and support the hypothesis that endogenous GLP-1R-expressing circuits are important “anticraving” pathways that when activated reduce drug seeking during abstinence. These results are consistent with a previous study in which we reported that chemogenetic activation of GLP-1-producing NTS neurons that project to the laterodorsal tegmental nucleus (LDTg) reduced cocaine seeking (15). These effects were mediated, in part, by activation of GLP-1Rs on GABAergic LDTg neurons that project to the VTA (15). Collectively, these findings indicate that activation of GLP-1-producing neurons in the NTS attenuates cocaine seeking and regulates the mesolimbic dopamine system via direct projections to the VTA as well as polysynaptic connections to the VTA via GLP-1R-expressing hubs such as the LDTg. It should be noted that the NTS consists of a heterogeneous population of cells and that other cell types may have been targeted by our viral approaches including noradrenergic cells that project to the VTA. Noradrenergic cells are activated by cocaine self-administration and could contribute to the suppressive effects of CNO-induced activation of NTS→VTA circuits on cocaine seeking during abstinence (28–31).

Previous studies in drug-naïve rodents showed that activation of GLP-1-producing NTS neurons that project to the VTA transiently reduced food intake (16). Consistent with these effects, systemic infusions of GLP-1R agonists attenuate food intake in drug-naïve rodents and humans (18, 19, 32). Therefore, we screened for these potential adverse effects following NTS→VTA circuit activation in our cocaine-experienced animals. We found that activation of NTS→VTA circuits suppressed cocaine seeking in rats without affecting ad libitum food and water intake. Thus, targeted activation of endogenous GLP-1-producing neural circuits selectively reduces drug seeking during abstinence in cocaine-experienced rats. Although it is not clear how these findings will translate to human cocaine users, these preclinical studies indicate that activation of NTS→VTA GLP-1-producing projections selectively reduced cocaine seeking. The potential weight loss effects of GLP-1R agonists, however, are of particular concern for stimulant users who may have preexisting malnutrition status. In addition to monitoring weight loss and nutritional status, future clinical trials should measure nausea and emesis following activation of central GLP-1-producing circuits as these adverse effects are a primary reason cited for discontinuation of GLP-1R agonist pharmacotherapy (17, 33).

To date, only one other study has investigated the functional role of NTS→VTA circuits in motivated behaviors. This study showed that chemogenetic activation of NTS→VTA projections decreased consumption of a high-fat diet (HFD) in drug-naïve mice (16). In contrast, our findings clearly show that chemogenetic activation of NTS→VTA projections during abstinence did not decrease ad libitum food intake or body weight in cocaine-experienced rats. These findings are consistent with our previous behavioral pharmacology studies in which we identified behaviorally selective doses of systemic and intra-VTA exendin-4 that reduced drug seeking in cocaine-experienced rats and did not reduce food intake or body weight (9). Although not clear, these discrepant findings could be due to species differences, cocaine exposure, and/or selective effects of NTS→VTA circuit activation on macronutrient preference (HFD versus normal chow). In support of the latter, chemogenetic activation of the NTS suppressed consumption of a HFD but did not suppress intake of normal chow in drug-naïve mice (16). A limitation of this study was the activation of heterogeneous NTS neuron populations (i.e., neither GLP-1-producing cells or projection-specific neurons were targeted). It is possible that additional satiety signals, such as glutamate (34), GABA (35), cholecystokinin (36), pro-opiomelanocortin (37), neuropeptide Y (38), and/or norepinephrine (28), are mediating the macronutrient-dependent feeding responses associated with NTS neuron activation. However, given that GLP-1R agonism in the VTA more robustly suppresses the intake of highly palatable foods compared to normal chow in drug-naïve rodents (27, 39, 40), it is likely that endogenous GLP-1 signaling in the VTA more selectively regulates hedonic rewards versus homeostatic signals (4). Our preclinical evidence to date indicate that cocaine-mediated behaviors are more sensitive to modulation by GLP-1R agonists and increased central GLP-1 signaling than nondrug motivated behaviors in cocaine-experienced rats. Notably, exenatide-based GLP-1R agonists have 53% structural homology to endogenous human GLP-1 (41), while semaglutide, a newer-generation GLP-1R agonist, has 94% structural homology to endogenous human GLP-1 and is less susceptible to degradation by dipeptidyl peptidase IV (42). Future preclinical studies should investigate the effects of these newer-generation GLP-1R agonists, which may have enhanced efficacy on cocaine seeking.

The efficacy of systemic GLP-1R agonists to attenuate cocaine seeking is associated with increased activity of GABA neurons in the VTA

While an emerging literature indicates that activation of VTA GLP-1Rs is sufficient to reduce drug-seeking behavior (9, 15), the cell type-specific neural mechanisms underlying the efficacy of GLP-1R agonists and increased GLP-1 signaling in the VTA on cocaine seeking remain largely unknown. Using FISH and snRNA-seq, we discovered that GLP-1Rs are expressed primarily on GABA neurons in the rat VTA. No *Glp1r* transcripts were identified in VTA dopamine neurons. This anatomy suggests that enhanced GLP-1 signaling in the VTA regulates cocaine seeking, in part, through activation of GLP-1Rs expressed on inhibitory midbrain circuits. These data are consistent with previous studies of transgenic mice modified to express fluorescent proteins under the *Glp1r* promoter (43, 44). These studies showed little to no coexpression GLP-1Rs and dopamine cell markers in the VTA (43, 44) and high coexpression of GLP-1Rs and GABA cell markers throughout the mesolimbic reward system (43). We also identified populations of *Glp1r*-expressing cells in the VTA

that did not express *Gad1* or *Th*. Future studies are needed to characterize these cell populations and determine their functional relevance to cocaine-mediated behaviors.

GLP-1Rs are coupled predominantly to G_s proteins and increase cAMP signaling when activated (45, 46). Electrophysiology studies in drug-naïve rodents revealed that GLP-1R agonism transiently increased the frequency and amplitude of spontaneous and miniature inhibitory postsynaptic currents (47–49). Together with our present findings that GLP-1Rs are expressed primarily on VTA GABA neurons and that GLP-1R agonism increases c-Fos expression in VTA neurons, we hypothesized that systemic administration of a GLP-1R agonist would increase the activity of VTA GABA neurons and decrease cocaine seeking. Here, we showed that exendin-4 increased VTA GABA neuron activity during cocaine seeking at a dose that significantly attenuated cocaine reinstatement. These findings highlight a mechanism wherein GLP-1R agonist pharmacotherapy activates inhibitory midbrain neurons to suppress cocaine-seeking behavior. These data are also consistent with our present studies showing chemogenetic activation of VTA GABA neurons attenuated cocaine seeking, as well as prior studies in which stimulation of GABA neurons in the VTA with GABA receptor agonists attenuated the ability of cocaine (50), cocaine-paired cues (51), and stress (52) to reinstate cocaine-seeking behavior. The current study is limited to the effects of GLP-1R activation on VTA GABA neuron activity during cocaine-primed reinstatement. Future studies are needed to determine whether GLP-1R pharmacotherapy has similar effects on VTA GABA neurons during cue-induced and/or stress-induced reinstatement. It is possible that the GLP-1R-expressing circuits that mediate the ability of these distinct stimuli to reinstate cocaine-seeking behavior are different. Given the high coexpression of GLP-1Rs and GABA cell markers throughout the mesolimbic system (15, 43), GABA neurons in other nuclei implicated in cocaine seeking are anatomically and functionally positioned to contribute to the efficacy of GLP-1R pharmacotherapy. Therefore, future studies should also explore how GLP-1R pharmacotherapy influences the activity of GABA neurons in other relevant nuclei, such as the LDTg, the central nucleus of the amygdala (CeA), and the NAc, as well as how these GLP-1R-expressing GABA circuits regulate cocaine-mediated behaviors.

Previously, we showed that systemic exendin-4 penetrates the brain and distributes to the VTA where it is localized in proximity to *Th*⁺ neurons (9). Anatomical studies, albeit in mice, identified dense GLP-1R-expressing fibers surrounding VTA dopamine neurons (43). These data suggest a presynaptic mechanism by which GLP-1R-expressing terminals are modulating phasic dopamine cell firing in the VTA. Activation of GLP-1Rs expressed on presynaptic terminals in the hippocampus has been shown to enhance depolarization-evoked GABA release (53). It is possible that GLP-1R agonists reduce cocaine seeking, in part, by increasing GABA release from presynaptic terminals in the VTA, effects consistent with the postsynaptic mechanism revealed in the current study. In addition, one study suggested that activating presynaptic GLP-1Rs may alter glutamate signaling in the VTA and, in turn, modulate midbrain dopamine cell activity (39). Thus, the neurochemical mechanisms in the midbrain underlying the efficacy of GLP-1R agonists on cocaine seeking are complex and likely involve both presynaptic and postsynaptic GLP-1Rs. Future studies are needed to fully characterize the role of presynaptic VTA GLP-1Rs in modulating phasic dopamine cell firing and cocaine-seeking behavior.

The efficacy of systemic GLP-1R agonists to attenuate cocaine seeking is associated with decreased activity of dopamine cells in the VTA

VTA dopamine neurons mediate the rewarding effects of cocaine, and increased dopamine cell firing in the VTA is necessary for cocaine seeking (54, 55). For example, chemogenetic inhibition of VTA dopamine neurons prevented the ability of a priming injection of cocaine and stress to reinstate drug seeking in cocaine-experienced rats (55). In addition, in vivo electrophysiology studies in awake, freely behaving rats have shown that cocaine increases VTA dopamine cell firing (56, 57), and cocaine self-administration produces long-term changes in VTA dopamine neuron excitability to drive cocaine seeking (58). In the current study, we showed that exendin-4 attenuates cocaine seeking and blocks cocaine seeking-evoked increases in VTA dopamine activity. These findings are consistent with microdialysis studies showing that systemic doses of exendin-4 that attenuated cocaine-induced conditioned place preference and cocaine self-administration in mice also decreased cocaine-evoked dopamine release in the NAc (21) and dorsal striatum (26). Similarly, a study done in head-fixed rats using fast-scan cyclic voltammetry showed that exendin-4 pretreatment suppressed the induction of phasic dopamine release events in the NAc by intravenous cocaine (59). Collectively, these findings suggest that increased GLP-1R activation in the VTA attenuates cocaine seeking, in part, by decreasing phasic dopamine cell firing. Future studies are needed to explore how GLP-1R agonism influences dopamine release in the striatum, as well as the activity of D1 dopamine receptor- and D2 dopamine receptor-expressing medium spiny neurons in the NAc during cocaine seeking. These studies will provide important insights into the how activation of GLP-1Rs in the VTA attenuates dopamine signaling to influence activity in the two main output pathways of the striatal complex and ultimately decrease cocaine seeking.

Comprehensively, our results indicate that GLP-1R agonist pharmacotherapy produces distinct cellular responses in VTA GABA and dopamine neurons of cocaine-experienced rats. Specifically, we found GLP-1R agonist pharmacotherapy increased VTA GABA neuron activity associated with cocaine seeking and suppressed cocaine seeking-evoked increases in VTA dopamine neuron activity. There are heterogeneous populations of GABA neurons in the VTA, including GABA interneurons. VTA GABA interneurons provide a local source of inhibitory control (60) and disrupt reward-mediated behaviors (61–63). Thus, our data suggest a neural mechanism by which GLP-1R agonists attenuate cocaine seeking through stimulation of local GABA neurons that suppress VTA dopamine cell firing (Fig. 7). In addition to GABA interneurons, we hypothesize that activation of presynaptic GLP-1Rs promotes GABA release onto VTA dopamine neurons to suppress their activity during cocaine seeking. Since VTA GABA neurons in the VTA have also been shown to be outwardly projecting, it is also possible that GLP-1Rs are expressed on GABA neurons in the VTA that project to downstream nuclei including the NAc, CeA, prefrontal cortex, lateral hypothalamus, and the lateral habenula (64–66). Future studies are needed to comprehensively characterize the anatomy of GLP-1R-expressing inhibitory midbrain circuits and their unique functional roles in cocaine-seeking behavior.

Here, we identified an endogenous GLP-1-producing neural circuit that regulates cocaine-seeking behavior. We also discovered a cell type-specific mechanism in the VTA underlying the efficacy of a GLP-1R agonist on cocaine seeking. These data highlight a potential therapeutic

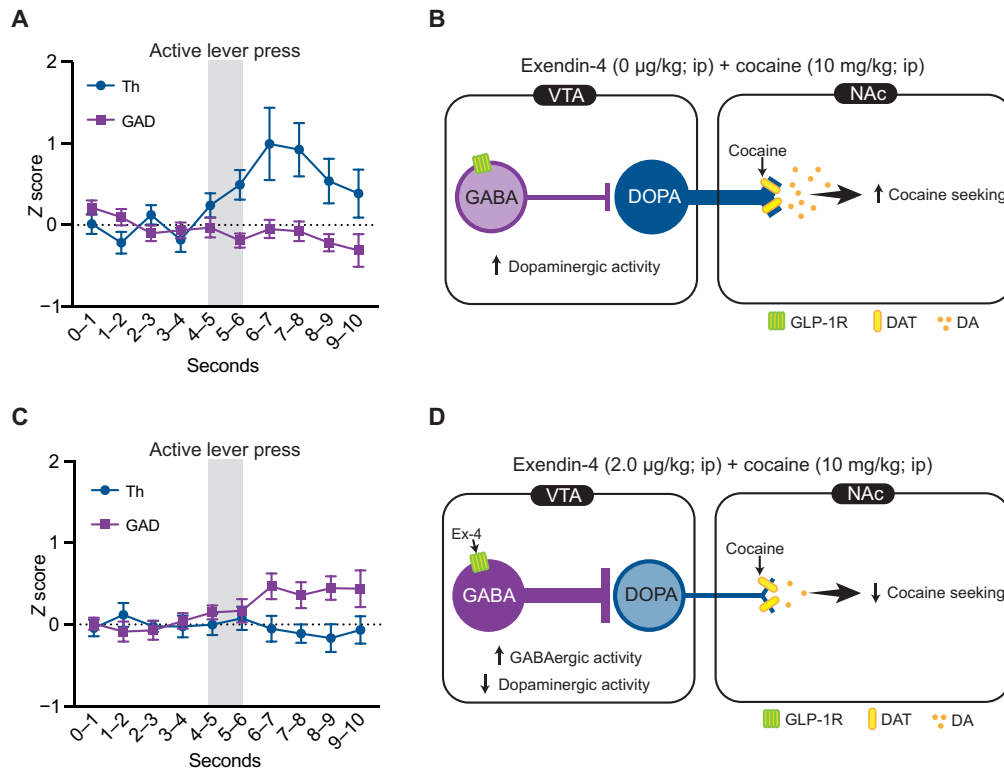


Fig. 7. GLP-1R agonist pharmacotherapy attenuates cocaine seeking by activating inhibitory VTA GABA neurons and decreasing activity of VTA dopamine neurons. (A) Normalized and down-sampled dopamine and GABA z score traces during cocaine seeking from rats pretreated with vehicle before cocaine priming-induced reinstatement test sessions. (B) Schematic illustrating cocaine seeking-evoked increases in dopamine cell firing in the VTA. (C) Normalized and down-sampled dopamine and GABA z score traces during cocaine seeking from rats pretreated with exendin-4 before cocaine priming-induced reinstatement test sessions. (D) Schematic illustrating one proposed mechanism by which exendin-4 increases VTA GABA cell firing which, in turn, inhibits VTA dopamine cell firing and suppresses cocaine-seeking behavior. Additional mechanisms likely include regulation of presynaptic GABA and/or glutamate release (see the main text for more details). DAT, dopamine transporter; DA, dopamine.

approach to targeting endogenous GLP-1-producing anticraving circuits to reduce cocaine relapse and further support of the translational potential of GLP-1R agonists as pharmacotherapies for CUD. Our findings also inform innovative strategies in the development of next-generation GLP-1R-based therapies to treat CUD. Studies in drug-naïve animals revealed that activation GLP-1-producing neurons in the NTS are not necessary for the anorexic effects of systemic GLP-1R agonists and that concurrent NTS GLP-1-producing circuit activation suppresses feeding more potently than GLP-1R agonism alone (67). Therefore, simultaneous activation of endogenous GLP-1-producing anticraving circuits and systemic GLP-1R agonist administration are a provocative therapeutic strategy that may suppress drug seeking to a greater degree than either intervention alone in cocaine-experienced rats.

MATERIALS AND METHODS

Animals and housing

Male Sprague-Dawley rats (*Rattus norvegicus*) weighing 225 to 250 g were obtained from Taconic Laboratories (Rensselaer, NY). Male and female transgenic Long-Evans rats (*Rattus norvegicus*) expressing Cre recombinase under the rat *Gad1* promoter [LE-Tg(*Gad1-iCre*)3Otc] were purchased from the Rat Resource and Research Center (RRRC P40OD011062; Columbia, MO) (15, 68, 69). Male and female transgenic

Sprague-Dawley rats (*Rattus norvegicus*) expressing Cre recombinase under the rat *Th* promoter [HsdSage:SD-*TH^{em1}*(*IRES-Cre*)Sage] were purchased from Envigo (Indianapolis, IN) (70, 71). Rats were housed individually on a 12/12-hour light/dark cycle and maintained on ad libitum food and water. All experimental procedures were performed during the light cycle. The experimental protocols were consistent with the guidelines issued by the US National Institutes of Health and were approved by the University of Pennsylvania's Institutional Animal Care and Use Committee (protocol #805705).

Drugs

Cocaine HCl was obtained from the National Institute on Drug Abuse (Rockville, MD) and dissolved in bacteriostatic 0.9% saline. Exendin-(9-39) and exendin-4 were purchased from Bachem (Torrance, CA) and dissolved in artificial cerebrospinal fluid (aCSF; Harvard Apparatus, Holliston, MA) and bacteriostatic 0.9% saline, respectively. CNO was obtained from Toronto Research Chemicals (North York, ON) and dissolved in 1% dimethyl sulfoxide in bacteriostatic 0.9% saline. Fluoro-exendin-4 was purchased from AnaSpec (Fremont, CA) and dissolved in bacteriostatic 0.9% saline. The doses and time courses of administration for each of the aforementioned compounds were based on the following experiments in rats: exendin-(9-39) (15), exendin-4 (9, 14, 72), CNO (15, 69), and fluoro-exendin-4 (19, 73).

Catheterization surgery

Rats were handled daily and allowed 1 week to acclimate to their home cages upon arrival. Before surgery, rats were anesthetized with ketamine (100 mg/kg; Midwest Veterinary Supply, Valley Forge, PA) and xylazine (10 mg/kg Sigma-Aldrich/RBI, St. Louis, MO). An indwelling catheter (SAI Infusion Technologies, Lake Villa, IL) was inserted into the right jugular vein and sutured in place. The catheter was routed to a mesh backmount that was implanted subcutaneously above the shoulder blades. To prevent infection and maintain patency, catheters were flushed daily with 0.2 ml of the antibiotic Timentin (0.93 mg/ml; Thermo Fisher Scientific, Pittsburgh, PA) dissolved in heparinized 0.9% saline (Butler Schein, Dublin, OH). When not in use, catheters were sealed with plastic obturators.

Cocaine self-administration, extinction, and the reinstatement of cocaine-seeking behavior

Rats were allowed 7 days to recover from surgery before behavioral testing commenced. Initially, rats were placed in operant conditioning chambers and allowed to lever-press for intravenous infusions of cocaine (0.245 mg/kg per infusion, infused more than 5 s) on a fixed-ratio 1 (FR1) schedule of reinforcement similar to our previous studies (9, 14, 15, 24). Rats were allowed to self-administer a maximum of 30 injections per 2-hour operant session. Once a rat achieved at least 20 infusions of cocaine in a single daily operant session under the FR1 schedule, the subject was switched to a fixed-ratio 5 (FR5) schedule of reinforcement. The maximum number of infusions was again limited to 30 per daily self-administration session under the FR5 schedule. For both FR1 and FR5 schedules, a 20-s timeout period followed each cocaine infusion, during which time active lever responses were tabulated but had no scheduled consequences. Responses made on the inactive lever, which had no scheduled consequences, were also recorded. Following 21 days of daily cocaine self-administration sessions, drug-taking behavior was extinguished by replacing the cocaine solution with 0.9% saline. Daily extinction sessions continued until responding on the active lever was <15% of the total active lever responses completed on the last day of cocaine self-administration. Typically, it took ~5 to 7 days for rats to meet this criterion. Once cocaine self-administration was extinguished, rats entered the reinstatement phase of the experiment. To reinstate cocaine-seeking behavior, rats received an acute priming injection of cocaine (10 mg/kg, ip) immediately before a 2-hour reinstatement test session (9, 14, 15). During reinstatement test sessions, satisfaction of the response requirement (i.e., five presses on the active lever) resulted in an infusion of saline. Using a between-sessions design, each reinstatement test session was followed by extinction sessions until responding was again <15% of the total active lever responses completed on the last day of cocaine self-administration. In general, 1 to 2 days of extinction were necessary to reach extinction criterion between reinstatement test sessions.

Blood collection and analysis

To determine the effects of cocaine taking and subsequent abstinence on circulating GLP-1 levels, a group of Sprague-Dawley rats underwent catheterization surgery and were then randomly assigned to one of two treatment groups: cocaine-experimental group or yoked saline controls. Cocaine-experimental rats were allowed to self-administer cocaine on an FR1 schedule of reinforcement for 21 days. Each rat that was allowed to respond for contingent cocaine infusions was paired with a yoked rat that received infusions of

saline. While lever pressing for the yoked saline rats had no scheduled consequences, these rats received the same number and temporal pattern of infusions as self-administered by their paired cocaine-experimental rat. Blood samples were collected from the tail immediately after operant sessions on self-administration day 21, extinction day 1, and extinction day 7. Blood was collected on ice into SAFE-T-FILL capillary collection tubes (RAM Scientific) containing protease and dipeptidyl peptidase IV inhibitors to prevent the rapid degradation of GLP-1. Blood samples were then centrifuged at 4°C for 10 min at 14,000 rpm (Centrifuge 5804R, Eppendorf). Plasma was aliquoted into Eppendorf tubes and stored at –80°C. Plasma GLP-1 concentrations were analyzed by an experimenter blinded to treatment conditions in the DRC Radioimmunoassay and Biomarkers Core at Penn using the Human GLP-1(7-36) ELISA Kit (ab184857; Abcam) according to manufacturer's instructions. Briefly, plasma was diluted 1:10 with sample diluent, and 50 µl each of diluted plasma and antibody cocktail solution were added to each well of a microplate. After 1-hour incubation at room temperature (RT), microplates were rinsed three times with wash buffer and then allowed to react with 100 µl of tetramethylbenzidine development solution for 15 min. Reactions were terminated by adding 100 µl of stop solution to each well, and fluorescence was measured using a ELx800 NB University Microplate Reader. Each sample was run in triplicate, and the assay sensitivity was 25 pg/ml. Mean GLP-1 levels are expressed as picograms per milliliter of plasma.

Chemogenetic activation of NTS→VTA projections in cocaine-experienced rats

To selectively target NTS→VTA projections, Sprague-Dawley rats underwent catheterization surgery and were immediately mounted in a stereotaxic apparatus (Kopf Instruments, CA). Rats received bilateral infusions of the retrogradely infecting CAV2-Cre directly into the VTA [–6.00 mm A/P, ±0.50 mm M/L, and –8.50 mm D/V relative to bregma according to the atlas of Paxinos and Watson (74)]. During the same surgical session, an AAV expressing a neural activating DREADD [AAV2-hSyn-DIO-hM3D(Gq)-mCherry] or control virus (AAV2-hSyn-DIO-mCherry) was infused bilaterally into the caudal NTS [–1.00 mm A/P relative to the occipital fissure, ±0.50 mm M/L, and –6.00 mm D/V relative to bregma according to the atlas of Paxinos and Watson (74)]. Both viruses were infused at a titer of 1×10^{12} gc/ml in a volume of 500 nl over 90 s. Microinjectors were left in place for an additional 90 s after infusion to allow for diffusion away from the injection sites. We have used this dual virus approach before to dissect the functional role of specific neural circuits in cocaine seeking (15). After a 14-day viral expression and recovery period, rats were allowed to self-administer cocaine for 21 days as described above. Once cocaine taking was extinguished, rats were pretreated with vehicle or CNO (0.1 or 1.0 mg/kg, ip) 30 min before an acute priming injection of cocaine (10 mg/kg, ip) similar to our previous reinstatement experiments in rats (15).

To determine whether the effects of activating NTS→VTA projections on cocaine seeking were due to increased GLP-1 signaling in the VTA, a subset of rats were implanted with bilateral VTA guide cannulae (26 gauge; 16 mm; Plastics One, Roanoke, VA) following viral infusions. Guide cannulae were implanted 2.0 mm dorsal to the VTA [–6.00 mm A/P, ±0.50 mm M/L, and –6.50 mm D/V relative to bregma according to Paxinos and Watson (74)] and cemented in place by affixing dental acrylic to stainless steel screws secured in the skull. An obturator (33 gauge; Plastics One) was inserted into

each guide cannula to prevent occlusion. On treatment days, micro-injectors that extended 2.0 mm past the ventral ends of the guide cannulae were used to infuse drugs directly into the VTA. Using a within subjects, counterbalanced design, rats were pretreated with bilateral infusions of vehicle or exendin-(9-39) (10 µg/100 nl) directly into the VTA 10 min before a systemic injection of vehicle or CNO (1.0 mg/kg, ip), similar to our previous experiments (15). The ability of intra-VTA exendin-(9-39) to block the effects of CNO on cocaine priming-induced reinstatement was assessed 30 min later.

Brains were dissected immediately following the last reinstatement test session. IHC was performed on coronal sections of the NTS to (i) visualize viral expression, (ii) quantify CNO-induced c-Fos expression in mCherry- and hM3D(Gq)-expressing neurons, and (iii) identify DREADD expression in GLP-1-positive NTS cells. Colocalization of mCherry and c-Fos following CNO treatment was quantified using three representative coronal sections of the NTS from each brain ($n = 3$ rats per treatment; three slices per rat). Missed cannula placements and/or lack of viral expression resulted in rats being excluded from subsequent data analyses.

Ad libitum food intake

GLP-1 is a satiety factor, and GLP-1R activation suppresses food intake in drug-naïve rodents (4, 18, 19). To screen for these potential feeding effects in our chemogenetic experiments, a subset of cocaine-experienced rats was housed in hanging wire cages with ad libitum access to food and water as described previously (9, 15, 72). After cocaine reinstatement test sessions, rats were immediately returned to the hanging wire cages and given ad libitum access to normal chow (5053, Pico Lab Rodent Diet 20; LabDiet, Richmond, IN). Food weights were measured 1, 3, 6, and 24 hours postsession (3, 5, 8, and 26 hours postvehicle or post-CNO injection). Body weight was measured 24 hours postsession (26 hours post-CNO injection) similar to our previous studies (15).

Verification of cannula placements

After completion of all microinjection experiments, rats were anesthetized with pentobarbital (100 mg/kg, ip). Brains were dissected and drop fixed in 10% formalin. Coronal sections (100 µm) were taken at the level of the VTA using a cryostat (Leica 3050S; Leica Corp., Deerfield, IL). An individual blinded to behavioral responses verified microinjection sites using light microscopy. Rats with cannula placements outside of the targeted brain region and/or excessive mechanical damage were excluded from subsequent data analyses.

Immunohistochemistry

Rats were deeply anesthetized with fatal plus (100 mg/kg, ip; Vortech Pharmaceuticals, Dearborn MI) and transcardially perfused with 0.1 M phosphate-buffered saline (PBS) (pH 7.4), followed with 4% formalin in 0.1 M PBS. Brains were removed, postfixed overnight in 4% formalin in 0.1 M PBS, and then cryoprotected in 20% sucrose in 0.1 M PBS at 4°C for 3 days. Coronal sections (30 µm) were taken using a cryostat (Leica 3050S; Leica Corp., Deerfield, IL). Brain sections were stored in 0.1 M PBS at 4°C until processed. IHC was performed on free-floating coronal sections containing the NTS or VTA according to modified procedures from previously published studies (15, 75). Briefly, sections were washed with 1% sodium borohydride followed by 0.1 M PBS. Sections were then blocked in 0.1 M PBS containing 5% normal donkey serum and 0.2% Triton X-100 for 1 hour at RT. Sections were incubated in primary antibodies

overnight and then, following a PBS rinse, incubated in secondary antibodies for 2 hours. The primary antibodies used were mouse anti-c-Fos (1:500; sc-271243, Santa Cruz Biotechnology Inc., Dallas, TX), rabbit anti-GLP-1 (1:1000; T-4363, Peninsula Laboratories International Inc., San Carlos, CA), and mouse anti-mCherry (1:1000; 632543, Takara, Kyoto, Japan). Secondary antibodies were donkey anti-mouse Alexa Fluor 488 (1:500), donkey anti-rabbit Alexa Fluor 488 (1:500), and donkey anti-mouse Alexa Fluor 594 (1:500) from Jackson ImmunoResearch (West Grove, PA). Sections were then washed and mounted onto glass slides and coverslipped using VECTASHIELD (Vector Laboratories; Burlingame, CA). Sections were visualized with a Leica SP5 X confocal microscope using the 63× oil-immersion objectives along with 488- and 594-nm laser lines. Image z-stacks were captured at the 63× oil-immersion objectives with a step size of 1 µm.

Electrophysiology validating CNO-induced DREADD activation of NTS cells

Rats expressing AAV2-hSyn-DIO-hM3D(Gq)-mCherry or AAV2-hSyn-DIO-mCherry in the NTS were deeply anesthetized with isoflurane and then quickly perfused with ice-cold cutting solution containing 92 mM *N*-methyl-D-glucamine, 2.5 mM KCl, 1.2 mM NaH₂PO₄, 30 mM NaHCO₃, 20 mM Hepes, 25 mM glucose, 5 mM sodium ascorbate, 2 mM thiourea, 3 mM sodium pyruvate, 10 mM MgSO₄, and 0.5 mM CaCl₂, saturated with carbogen (95% O₂/5% CO₂) (pH 7.4) with HCl and an osmolarity of 305 to 315 mOsm (76). Following decapitation, brains were removed for dissection, and horizontal slices (250-µm thick) of the NTS were obtained using a VT1000S vibratome (Leica, Weltzar, Germany). Slices were made at 4°C, then transferred to a holding chamber with the same cutting solution, and incubated at 37°C for 10 to 12 min. Slices were then moved to a beaker of RT holding ACSF containing 86 mM NaCl, 2.5 mM KCl, 1.2 mM NaH₂PO₄, 35 mM NaHCO₃, 20 mM Hepes, 25 mM glucose, 5 mM sodium ascorbate, 2 mM thiourea, 3 mM sodium pyruvate, 1 mM MgCl₂, and 2 mM CaCl₂ and saturated with carbogen (pH 7.3 to 7.4) and an osmolarity of 305 to 315 mOsm. Slices were allowed to recover for at least 45 min before performing recordings.

Slices were transferred to a Nikon Eclipse FN1 upright microscope equipped for differential interference contrast infrared optics. The recording chamber was continuously perfused with oxygenated recording ACSF containing 119 mM NaCl, 2.5 mM KCl, 26 mM NaHCO₃, 1.2 mM NaH₂PO₄, 12.5 mM glucose, 5 mM Hepes, 1 mM MgSO₄, and 2 mM CaCl₂ (pH 7.3 to 7.4) and an osmolarity of 305 to 315 mOsm. The solution was heated to 32° ± 1°C using an automatic temperature controller (Warner Instruments). The NTS was identified using a 5× objective, and individual neurons were magnified with a 40× water immersion lens. DREADD-positive neurons were further identified by fluorescence with a DS-Red filter (Nikon). Recording pipettes were pulled from borosilicate glass capillaries (World Precision Instruments) to a resistance of 3.8 to 5.0 megohm when filled with intracellular solution. The intracellular solution contained the following: 145 mM potassium gluconate, 2.5 mM KCl, 2.5 mM NaCl, 0.1 mM 1,2-bis(2-aminophenoxy)ethane-*N,N,N',N'*-tetraacetic acid, 10 mM Hepes, 1.0 mM L-glutathione, 7.5 mM sodium phosphocreatine, 2.0 mM Mg-adenosine triphosphate, and 0.25 mM tris-guanosine triphosphate (pH 7.2 to 7.3) with KOH and an osmolarity of 285 to 295 mOsm. All recordings were performed in whole-cell current-clamp mode using a MultiClamp 700B amplifier. Baseline spontaneous firing was recorded for ≥5 min before

the activation of DREADD-positive neurons by CNO (30 μ M) dissolved in the recording ACSF. After ≥ 5 min, CNO was washed out with regular recording ACSF. All recordings were low-pass-filtered at 3 kHz, amplified five times, and then digitized at 20 kHz using a Digidata 1440A acquisition board and pClamp10 software (both from Molecular Devices). For all experiments, access resistance was 15 to 25 megohm, uncompensated, and monitored continuously during recording. Cells with a change in access resistance $>20\%$ over the course of data acquisition were not accepted for data analysis.

Fluorescence in situ hybridization

FISH was used to quantify cell type-specific *Glp1r* expression in the VTA of drug-naïve, wild-type Long Evans rats ($n = 3$ rats) and verify cell type-specific GCaMP8f expression in transgenic rats used in the fiber photometry experiments ($n = 4$ rats; two rats per transgenic line). Brains were dissected, flash frozen in -20°C isopentane, and stored at -80°C . Using a cryostat (Leica 3050S; Leica Corp., Deerfield, IL), coronal sections (8 μ m) were taken at the level of the VTA and immediately mounted onto Superfrost Plus slides (Thermo Fisher Scientific). *Glp1r*, *Th*, and *Gad1* mRNA transcripts were detected using the RNAScope Multiplex Fluorescent Reagent Kit V2 [catalog no. 320850; Advanced Cell Diagnostics (ACD), Hayward, CA] per the manufacturer's protocol. Slide mounted sections were rinsed in 10% formaldehyde for 15 min at 4°C . Following dehydration in ascending concentrations of ethanol solutions (5-min washes in 50, 70, and 100% ethanol), slides were air-dried, and a hydrophobic barrier was created around the sections using a hydrophobic pen (Vector Labs). The sections were then rinsed with PBS and treated with Protease IV (ACD, Hayward, CA) for 30 min at RT (followed by two 1-min rinses in PBS).

Pretreated tissue sections were processed immediately using probes designed by ACD to detect *Glp1r* (Rn-Glp1r-C1; 315221) or *eGfp* (EGFP; 400281-C1), *Gad1* (Rn-Gad1-C2; 316401-C2), and *Th* (Rn-Th-C3; 314651-C3) transcripts. Sections were incubated in a cocktail containing probes (Probe dilution: 50C1:1C2:1C3) for 2 hours at 40°C in a HybEZTM oven (ACD). Following signal amplification, opal dyes [Opal 520 (OP-001001), Opal 570 (OP-001003), and Opal 690 (OP-001006) (Akoya, Marlborough, MA)] were diluted in trichostatin A buffer (1:1000) and applied to the sections. After the final wash, slides were coverslipped using fluorogel mounting medium with 4',6-diamidino-2-phenylindole (DAPI; Thermo Fisher Scientific). Brain sections at four levels relative to bregma (-5.30 , -5.60 , -6.04 , and -6.30 mm A/P) were sampled from each rat. A total of four images (one image per level) from each rat were captured with a Keyence fluorescence microscope using the 10 \times , 20 \times , and 60 \times oil-immersion objectives. Image z-stacks were collected with a step size of 2 μ m. To quantify *Glp1r* expression in *Gad1*- and *Th*-expressing cells, the number of cells colabeled for *Glp1r* and *Gad1* transcripts or *Th* transcripts in 10 \times images were counted at each level per rat and totaled ($n = 3$ rats; four slices per rat). These numbers were divided by the total number of cells that expressed *Glp1r* to calculate the percentage of *Glp1r*-expressing cells that coexpress *Gad1* and/or *Th* transcripts at different A/P levels and in total. The number of cells expressing *Gad1* or *Th* transcripts was also counted at each level to quantify the total number of *Th*- and *Gad*-expressing cells in the VTA.

Single-nuclei RNA sequencing

Adult male Sprague-Dawley rats ($n = 5$) were rapidly decapitated, their brains were removed and flash-frozen in dry ice-cold isopentane.

Bilateral VTA punches were prepared on a cryostat and combined into a single sample. Nuclei were isolated from the samples as described previously (77, 78). Nuclei were processed for the 10x Genomics 3' gene expression assay (v3.1) and sequenced per the manufacturer's protocols. Raw sequencing data were processed and aligned to the rat reference genome as described previously (79). Downstream analyses of count data were performed with Seurat v4.3.0. Nuclei with mitochondrial transcript fractions $\geq 5\%$ or with ≤ 200 genes detected were removed, and the remaining nuclei were clustered at a resolution of 0.1. Count matrices were then corrected for cell-free mRNA background noise using SoupX v1.6.2, and nuclei with ≥ 5000 genes detected in the corrected data were removed. Count data were then normalized with SCTransform, and all samples were integrated with Seurat. Doublets were identified with scDblFinder v1.12.0 and removed. Clusters with low UMI or displaying markers for more than one major cell type were also removed. The final dataset was clustered at a resolution of 0.08 using the first 10 principal components based on highly variably expressed genes, and clusters were assigned to major cell types based on known marker genes.

Dual-wavelength in vivo fiber photometry recordings

Light-emitting diodes (LEDs; 465 and 405 nm; Tucker Davis Technologies (TDT), Alachua, FL) were used simultaneously in each rat to excite GCaMP8f and measure intracellular Ca^{2+} dynamics. The 465-nm LED excites (signal) calcium-dependent GCaMP8f fluorescence to provide a proxy for neural activity, while the 405-nm LED (isosbestic) excites calcium-independent GCaMP8f fluorescence to control for movement and fiber bleaching. The intensities of the 465- and 405-nm LEDs were sinusoidally modulated at 210 and 330 Hz, respectively. Both LED light sources were coupled to a dichroic mirror containing filter cube (FMC4, Doric Lenses, Quebec, Canada) and converged onto a fiber optical patch cord (Doric Lenses) attached to a ferule-capped optic implant (Doric Lenses). The emitted 510-nm fluorescent signal was collected through the same fiber optic patch cord coupled to the LEDs and filtered before being collected and amplified by a lock-in amplifier at an acquisition rate of 6 Hz (RZ10x, TDT). Using the iCON control interface and Synapse recording software (TDT), the RZ processor was integrated with operant chambers to record from freely moving rats during cocaine reinstatement test sessions. A custom closed-loop experiment was designed in Pynapse (TDT), a Python-based programming environment, to conduct drug-seeking experiments, record data, and time stamp behavioral events (e.g., lever presses).

Measuring cell type-specific Ca^{2+} dynamics in VTA neurons during cocaine reinstatement

To identify the midbrain mechanisms underlying the efficacy of exendin-4 on cocaine seeking, transgenic rats expressing Cre recombinase under the *Gad1* or *Th* promoter were implanted with indwelling jugular catheters as described above. A Cre-dependent GCaMP8f virus (AAV9-Syn-Flex-GCaMP8f-WPRE-SV40) was infused directly into the VTA (*Th* rats: -6.00 mm A/P, ± 0.50 mm M/L, and -8.50 mm D/V; *Gad1* rats: -6.30 mm A/P, ± 0.50 mm M/L, and -8.50 mm D/V). These coordinates were based on subregion- and cell type-specific patterns of *Gad1* and *Th* expression in the VTA (fig. S8, A and B). Viruses were infused unilaterally in a volume of 1 μ l over 5 min (titer = 1.0×10^{12} gc/ml). Microinjectors were left in place for an additional 5 min after infusion to allow for diffusion away from the injection

sites. A ferrule-capped optic fiber (Doric Lenses) was implanted 10 μm above the viral injection site (*Th* rats: -6.00 mm A/P , $\pm 0.50\text{ mm M/L}$, and -8.49 mm D/V ; *Gad1* rats: -6.30 mm A/P , $\pm 0.50\text{ mm M/L}$, and -8.49 mm D/V) and secured to the skull with Metabond cement (Parkell) and dental acrylic.

After a 14-day viral expression and recovery period, rats were allowed to self-administer cocaine as described above. Drug taking was then extinguished by replacing cocaine with saline. Once cocaine taking was extinguished, rats were pretreated with vehicle or exendin-4 (2.0 $\mu\text{g/kg}$, ip) 10 min before a priming injection of cocaine (10 mg/kg, ip). The dose of exendin-4 tested was shown previously to reduce drug taking in cocaine-experienced rats (9). Following the acute priming injection of cocaine, a fiber optic patch cord was secured to the optic fiber-containing ferrule implant. Rats were then placed immediately into the operant chambers, and drug seeking was assessed during a 2-hour reinstatement test session. Calcium-dependent GCaMP8f fluorescence was recorded for the first 30 min of the 2-hour reinstatement test session, and lever-dependent behavioral events were timestamped using the iCON control interface and Pynapse (TDT). Signals associated with the first three response requirements completed (i.e., the 5th, 10th, and 15th active lever presses) were analyzed in this study. Signals associated with inactive lever presses were also recorded and analyzed. Cell type-specific Ca^{2+} responses were also measured in separate rats that self-administered saline to determine whether the observed effects on calcium dynamics were specific to cocaine-seeking behavior and not due to handling and/or exposure to the operant chambers.

Fiber photometry data analysis

Raw signal (465 nm) and isosbestic control (405 nm) channel data were exported from Synapse to a CSV file using a MATLAB script provided by TDT. Custom R scripts were then used to independently process each trace (<https://zenodo.org/records/13984378>). First, the scale of channels was normalized using a least-squares regression to find the relationship between the signal and the control channel. The returning slope and the intercept were used to generate a scaled control channel. $\Delta F/F$ was then generated by subtracting the fitted isosbestic control channel from the signal channel to eliminate any movement or bleaching artifacts. To identify changes in fluorescence associated with cocaine seeking, time stamps were used to divide the processed trace into 10-s trials. Trials were z scored to a baseline period defined as 5 s before engagement with the operant box levers.

Chemogenetic activation of VTA GABA neurons in cocaine-experienced rats

To selectively activate VTA GABA neurons, transgenic male rats expressing Cre recombinase under the *Gad1* promoter were implanted with indwelling jugular catheters as described above. A virus expressing a Cre-dependent neural activating DREADD [AAV2-hSyn-DIO-hM3D(Gq)-mCherry] was infused bilaterally into the VTA (-6.00 mm A/P , $\pm 0.50\text{ mm M/L}$, and -8.50 mm D/V) in a volume of 500 μl over 90 s (titer = $1.0 \times 10^{12}\text{ gc/ml}$). Microinjectors were left in place for an additional 90 s after infusion to allow for diffusion away from the injection sites. After a 14-day viral expression and recovery period, rats were allowed to self-administer cocaine for 21 days as described above. Once cocaine taking was extinguished, rats were pretreated with vehicle or CNO (0.1 or 1.0 mg/kg, ip) 30 min before an acute priming injection of cocaine (10 mg/kg, ip) similar

to our previous reinstatement experiments in rats (15). Rats were perfused, and brains were dissected immediately following the last reinstatement test session. IHC was used to visualize viral expression and CNO-induced c-Fos expression in hM3D(Gq)-expressing neurons. FISH was performed on 12- μm coronal sections of the VTA before IHC to identify DREADD expression in *Gad1*-positive cells. Following the dehydration steps described above, slides were washed three to five times in RT diH₂O and then for 10 s in hot diH₂O to acclimate and subsequently incubated in hot 1 \times TRR (322000, ACD) for 5 min according to the manufacturer's instructions. Slides were rinsed in RT diH₂O for 15 s and then transferred to 100% EtOH for 3 min. Slides were then air dried and a hydrophobic barrier was drawn around the sections using a hydrophobic pen (Vector Labs). The sections were then treated with Protease III (ACD, catalog no. 322337) for 30 min at RT followed by an RT diH₂O wash. FISH was then performed using the same protocol described above to detect *Gad1* mRNA transcripts, and IHC was performed to detect hM3D(Gq) expression using mouse anti-mCherry (1:1000; 632543, Takara).

Statistics

For all cocaine reinstatement experiments, total active and inactive lever responses were analyzed with repeated measures (RM) two-way mixed-factors analyses of variance (ANOVAs). Cumulative food intake data were also analyzed with RM two-way mixed-factors ANOVAs. For fiber photometry experiments, AUC and maximum z scores were analyzed with separate RM two-way mixed-factors ANOVAs. Pairwise analyses were made using Bonferroni post hoc tests ($P < 0.05$). Findings from all other experiments were analyzed using two-tailed, paired or unpaired t tests ($P < 0.05$).

Supplementary Materials

The PDF file includes:

Figs. S1 to S8

Legend for data file S1

Other Supplementary Material for this manuscript includes the following:

Data file S1

REFERENCES AND NOTES

1. K. Gangu, A. Bobba, S. D. Basida, S. Avula, H. Chela, S. Singh, Trends of cocaine use and manifestations in hospitalized patients: A cross-sectional study. *Cureus* **14**, e22090 (2022).
2. M. Kariisa, N. L. Davis, S. Kumar, P. Seth, C. L. Mattson, F. Chowdhury, C. M. Jones, Vital signs: Drug overdose deaths, by selected sociodemographic and social determinants of health characteristics - 25 states and the district of Columbia, 2019-2020. *MMWR Morb. Mortal Wkly. Rep.* **71**, 940-947 (2022).
3. S. E. Swinford-Jackson, C. P. O'Brien, P. J. Kenny, L. Vanderschuren, E. M. Unterwald, R. C. Pierce, The persistent challenge of developing addiction pharmacotherapies. *Cold Spring Harb. Perspect. Med.* **11**, a040311 (2021).
4. M. R. Hayes, H. D. Schmidt, GLP-1 influences food and drug reward. *Curr. Opin. Behav. Sci.* **9**, 66-70 (2016).
5. N. S. Hernandez, H. D. Schmidt, Central GLP-1 receptors: Novel molecular targets for cocaine use disorder. *Physiol. Behav.* **206**, 93-105 (2019).
6. R. Merkel, A. Moreno, Y. Zhang, R. Herman, J. Ben Nathan, S. Zeb, S. Rahematpura, K. Stecyk, B. T. Milliken, M. R. Hayes, R. P. Doyle, H. D. Schmidt, A novel approach to treating opioid use disorders: Dual agonists of glucagon-like peptide-1 receptors and neuropeptide Y(2) receptors. *Neurosci. Biobehav. Rev.* **131**, 1169-1179 (2021).
7. E. Jerlhag, The therapeutic potential of glucagon-like peptide-1 for persons with addictions based on findings from preclinical and clinical studies. *Front. Pharmacol.* **14**, 1063033 (2023).
8. B. Jones, The therapeutic potential of GLP-1 receptor biased agonism. *Br. J. Pharmacol.* **179**, 492-510 (2022).

9. N. S. Hernandez, K. Y. Ige, E. G. Miettlicki-Baase, G. C. Molina-Castro, C. A. Turner, M. R. Hayes, H. D. Schmidt, Glucagon-like peptide-1 receptor activation in the ventral tegmental area attenuates cocaine seeking in rats. *Neuropsychopharmacology* **43**, 2000–2008 (2018).
10. I. Merchenthaler, M. Lane, P. Shughrue, Distribution of pre-pro-glucagon and glucagon-like peptide-1 receptor messenger RNAs in the rat central nervous system. *J. Comp. Neurol.* **403**, 261–280 (1999).
11. E. Farkas, A. Szilvasy-Szabo, Y. Ruska, R. Sinko, M. G. Rasch, T. Egebjerg, C. Pyke, B. Gereben, L. B. Knudsen, C. Fekete, Distribution and ultrastructural localization of the glucagon-like peptide-1 receptor (GLP-1R) in the rat brain. *Brain Struct. Funct.* **226**, 225–245 (2021).
12. L. Rinaman, Ascending projections from the caudal visceral nucleus of the solitary tract to brain regions involved in food intake and energy expenditure. *Brain Res.* **1350**, 18–34 (2010).
13. H. J. Grill, M. R. Hayes, Hindbrain neurons as an essential hub in the neuroanatomically distributed control of energy balance. *Cell Metab.* **16**, 296–309 (2012).
14. N. S. Hernandez, B. O'Donovan, P. I. Ortinski, H. D. Schmidt, Activation of glucagon-like peptide-1 receptors in the nucleus accumbens attenuates cocaine seeking in rats. *Addict Biol.* **24**, 170–181 (2019).
15. N. S. Hernandez, V. R. Weir, K. Ragnini, R. Merkel, Y. Zhang, K. Mace, M. T. Rich, R. Christopher Pierce, H. D. Schmidt, GLP-1 receptor signaling in the laterodorsal tegmental nucleus attenuates cocaine seeking by activating GABAergic circuits that project to the VTA. *Mol. Psychiatry* **26**, 4394–4408 (2021).
16. X. F. Wang, J. J. Liu, J. Xia, J. Liu, V. Mirabella, Z. P. Pang, Endogenous glucagon-like peptide-1 suppresses high-fat food intake by reducing synaptic drive onto mesolimbic dopamine neurons. *Cell Rep.* **12**, 726–733 (2015).
17. M. V. Sikirica, A. A. Martin, R. Wood, A. Leith, J. Piercy, V. Higgins, Reasons for discontinuation of GLP1 receptor agonists: Data from a real-world cross-sectional survey of physicians and their patients with type 2 diabetes. *Diabetes Metab. Syndr. Obes.* **10**, 403–412 (2017).
18. M. R. Hayes, S. E. Kanoski, A. L. Alhadeff, H. J. Grill, Comparative effects of the long-acting GLP-1 receptor ligands, liraglutide and exendin-4, on food intake and body weight suppression in rats. *Obesity* **19**, 1342–1349 (2011).
19. S. E. Kanoski, L. E. Rupprecht, S. M. Fortin, B. C. De Jonghe, M. R. Hayes, The role of nausea in food intake and body weight suppression by peripheral GLP-1 receptor agonists, exendin-4 and liraglutide. *Neuropharmacology* **62**, 1916–1927 (2012).
20. J. L. Gomez, J. Bonaventura, W. Lesniak, W. B. Mathews, P. Sysa-Shah, L. A. Rodriguez, R. J. Ellis, C. T. Richie, B. K. Harvey, R. F. Dannals, M. G. Pomper, A. Bonci, M. Michaelides, Chemogenetics revealed: DREADD occupancy and activation via converted clozapine. *Science* **357**, 503–507 (2017).
21. E. Egicioglu, J. A. Engel, E. Jerlhag, The glucagon-like peptide 1 analogue, exendin-4, attenuates the rewarding properties of psychostimulant drugs in mice. *PLOS ONE* **8**, e69010 (2013).
22. H. D. Schmidt, S. M. Anderson, R. C. Pierce, Stimulation of D1-like or D2 dopamine receptors in the shell, but not the core, of the nucleus accumbens reinstates cocaine-seeking behaviour in the rat. *Eur. J. Neurosci.* **23**, 219–228 (2006).
23. F. M. Vassoler, H. D. Schmidt, M. E. Gerard, D. A. Ciraulo, C. Kornetsky, C. M. Knapp, R. C. Pierce, Deep brain stimulation of the nucleus accumbens shell attenuates cocaine priming-induced reinstatement of drug seeking in rats. *J. Neurosci.* **28**, 8735–8739 (2008).
24. H. D. Schmidt, E. G. Miettlicki-Baase, K. Y. Ige, J. J. Maurer, D. J. Reiner, D. J. Zimmer, D. S. Van Nest, L. A. Guercio, M. E. Wimmer, D. R. Olivos, B. C. De Jonghe, M. R. Hayes, Glucagon-like peptide-1 receptor activation in the ventral tegmental area decreases the reinforcing efficacy of cocaine. *Neuropsychopharmacology* **41**, 1917–1928 (2016).
25. S. Bouhhal, K. N. Ellefsen, M. B. Sheskie, E. Singley, S. Pirard, D. A. Gorelick, M. A. Huestis, L. Leggio, Acute effects of intravenous cocaine administration on serum concentrations of ghrelin, amylin, glucagon-like peptide-1, insulin, leptin and peptide YY and relationships with cardiorespiratory and subjective responses. *Drug Alcohol Depend.* **180**, 68–75 (2017).
26. G. Sorensen, I. A. Reddy, P. Weikop, D. L. Graham, G. D. Stanwood, G. Wortwein, A. Galli, A. Fink-Jensen, The glucagon-like peptide 1 (GLP-1) receptor agonist exendin-4 reduces cocaine self-administration in mice. *Physiol. Behav.* **149**, 262–268 (2015).
27. A. L. Alhadeff, L. E. Rupprecht, M. R. Hayes, GLP-1 neurons in the nucleus of the solitary tract project directly to the ventral tegmental area and nucleus accumbens to control for food intake. *Endocrinology* **153**, 647–658 (2012).
28. L. Rinaman, Hindbrain noradrenergic A2 neurons: Diverse roles in autonomic, endocrine, cognitive, and behavioral functions. *Am. J. Physiol. Regul. Integr. Comp. Physiol.* **300**, R222–R235 (2011).
29. D. M. Buffalari, L. Rinaman, Cocaine self-administration and extinction alter medullary noradrenergic and limbic forebrain cFos responses to acute, noncontingent cocaine injections in adult rats. *Neuroscience* **281**, 241–250 (2014).
30. S. Murphy, M. Collis Glynn, T. N. Dixon, H. J. Grill, G. P. McNally, Z. Y. Ong, Nucleus of the solitary tract A2 neurons control feeding behaviors via projections to the paraventricular hypothalamus. *Neuropsychopharmacology* **48**, 351–361 (2023).
31. W. B. Solecki, K. Szklarczyk, K. Pradel, K. Kwiatkowska, G. Dobrzański, R. Przewlocki, Noradrenergic signaling in the VTA modulates cocaine craving. *Addict Biol.* **23**, 596–609 (2018).
32. P. M. O'Neil, A. L. Birkenfeld, B. McGowan, O. Mosenzon, S. D. Pedersen, S. Wharton, C. G. Carson, C. H. Jepsen, M. Kabisch, J. P. H. Wilding, Efficacy and safety of semaglutide compared with liraglutide and placebo for weight loss in patients with obesity: A randomised, double-blind, placebo and active controlled, dose-ranging, phase 2 trial. *Lancet* **392**, 637–649 (2018).
33. M. E. Lean, R. Carraro, N. Finer, H. Hartvig, M. L. Lindegaard, S. Rossner, L. Van Gaal, A. Astrup, Tolerability of nausea and vomiting and associations with weight loss in a randomized trial of liraglutide in obese, non-diabetic adults. *Int. J. Obes. (Lond)* **38**, 689–697 (2014).
34. H. Zheng, R. L. Stornetta, K. Agassandian, L. Rinaman, Glutamatergic phenotype of glucagon-like peptide 1 neurons in the caudal nucleus of the solitary tract in rats. *Brain Struct. Funct.* **220**, 3011–3022 (2015).
35. M. Y. Shi, L. F. Ding, Y. H. Guo, Y. X. Cheng, G. Q. Bi, P. M. Lau, Long-range GABAergic projections from the nucleus of the solitary tract. *Mol. Brain* **14**, 38 (2021).
36. W. Qiu, C. R. Hutch, Y. Wang, J. Wloszek, R. A. Rucker, M. G. Myers, D. Sandoval, Multiple NTS neuron populations cumulatively suppress food intake. *Elife* **12**, e85640 (2023).
37. C. Zhan, J. Zhou, Q. Feng, J. E. Zhang, S. Lin, J. Bao, P. Wu, M. Luo, Acute and long-term suppression of feeding behavior by POMC neurons in the brainstem and hypothalamus, respectively. *J. Neurosci.* **33**, 3624–3632 (2013).
38. J. Chen, M. Cheng, L. Wang, L. Zhang, D. Xu, P. Cao, F. Wang, H. Herzog, S. Song, C. Zhan, A vagal-NTS neural pathway that stimulates feeding. *Curr. Biol.* **30**, 3986–3998.e5 (2020).
39. E. G. Miettlicki-Baase, P. I. Ortinski, L. E. Rupprecht, D. R. Olivos, A. L. Alhadeff, R. C. Pierce, M. R. Hayes, The food intake-suppressive effects of glucagon-like peptide-1 receptor signaling in the ventral tegmental area are mediated by AMPA/kainate receptors. *Am. J. Physiol. Endocrinol. Metab.* **305**, E1367–E1374 (2013).
40. S. L. Dickson, R. H. Shirazi, C. Hansson, F. Bergquist, H. Nissbrandt, K. P. Skibicka, The glucagon-like peptide 1 (GLP-1) analogue, exendin-4, decreases the rewarding value of food: A new role for mesolimbic GLP-1 receptors. *J. Neurosci.* **32**, 4812–4820 (2012).
41. J. Eng, W. A. Kleinman, L. Singh, G. Singh, J. P. Raufman, Isolation and characterization of exendin-4, an exendin-3 analogue, from Heloderma suspectum venom. Further evidence for an exendin receptor on dispersed acini from guinea pig pancreas. *J. Biol. Chem.* **267**, 7402–7405 (1992).
42. J. Lau, P. Bloch, L. Schaffer, I. Pettersson, J. Spetzler, J. Kofoed, K. Madsen, L. B. Knudsen, J. McGuire, D. B. Steensgaard, H. M. Strauss, D. X. Gram, S. M. Knudsen, F. S. Nielsen, P. Thygesen, S. Reedtz-Runge, T. Kruse, Discovery of the once-weekly glucagon-like peptide-1 (GLP-1) analogue semaglutide. *J. Med. Chem.* **58**, 7370–7380 (2015).
43. D. L. Graham, H. H. Durai, T. S. Trammell, B. L. Noble, D. P. Mortlock, A. Galli, G. D. Stanwood, A novel mouse model of glucagon-like peptide-1 receptor expression: A look at the brain. *J. Comp. Neurol.* **528**, 2445–2470 (2020).
44. S. C. Cork, J. E. Richards, M. K. Holt, F. M. Gribble, F. Reimann, S. Trapp, Distribution and characterisation of Glucagon-like peptide-1 receptor expressing cells in the mouse brain. *Mol. Metab.* **4**, 718–731 (2015).
45. J. J. Holst, The physiology of glucagon-like peptide 1. *Physiol. Rev.* **87**, 1409–1439 (2007).
46. D. J. Drucker, J. F. Habener, J. J. Holst, Discovery, characterization, and clinical development of the glucagon-like peptides. *J. Clin. Invest.* **127**, 4217–4227 (2017).
47. S. V. Korol, Z. Jin, O. Babateen, B. Birnir, GLP-1 and exendin-4 transiently enhance GABAA receptor-mediated synaptic and tonic currents in rat hippocampal CA3 pyramidal neurons. *Diabetes* **64**, 79–89 (2015).
48. I. Farkas, C. Vastagh, E. Farkas, F. Balint, K. Skrapits, E. Hrabovszky, C. Fekete, Z. Liposits, Glucagon-like peptide-1 excites firing and increases GABAergic miniature postsynaptic currents (mIPSCs) in gonadotropin-releasing hormone (GnRH) neurons of the male mice via activation of nitric oxide (NO) and suppression of endocannabinoid signaling pathways. *Front. Cell. Neurosci.* **10**, 214 (2016).
49. V. Chuong, M. Farokhnia, S. Khom, C. L. Pince, S. K. Elvig, R. Vilkolinsky, R. C. Marchette, G. F. Koob, M. Roberto, L. F. Vendruscolo, L. Leggio, The glucagon-like peptide-1 (GLP-1) analogue semaglutide reduces alcohol drinking and modulates central GABA neurotransmission. *JCI Insight* **8**, e170671 (2023).
50. K. McFarland, P. W. Kalivas, The circuitry mediating cocaine-induced reinstatement of drug-seeking behavior. *J. Neurosci.* **21**, 8655–8663 (2001).
51. P. Di Ciano, B. J. Everitt, Contribution of the ventral tegmental area to cocaine-seeking maintained by a drug-paired conditioned stimulus in rats. *Eur. J. Neurosci.* **19**, 1661–1667 (2004).
52. K. McFarland, S. B. Davidge, C. C. Lapish, P. W. Kalivas, Limbic and motor circuitry underlying footshock-induced reinstatement of cocaine-seeking behavior. *J. Neurosci.* **24**, 1551–1560 (2004).

53. C. Rebosio, M. Balbi, M. Passalacqua, R. Ricciarelli, E. Fedele, Presynaptic GLP-1 receptors enhance the depolarization-evoked release of glutamate and GABA in the mouse cortex and hippocampus. *Biofactors* **44**, 148–157 (2018).
54. W. Solecki, M. Wilczkowski, K. Pradel, K. Karwowska, M. Kielbinski, G. Drwięga, K. Zajda, T. Błasiak, Z. Soltys, Z. Rajfur, K. Szklarczyk, R. Przewlocki, Effects of brief inhibition of the ventral tegmental area dopamine neurons on the cocaine seeking during abstinence. *Addict. Biol.* **25**, e12826 (2020).
55. S. V. Mahler, Z. D. Brodnik, B. M. Cox, W. C. Buchta, B. S. Bentzley, J. Quintanilla, Z. A. Cope, E. C. Lin, M. D. Riedy, M. D. Scofield, J. Messinger, C. M. Ruiz, A. C. Riegel, R. A. España, G. Aston-Jones, Chemogenetic manipulations of ventral tegmental area dopamine neurons reveal multifaceted roles in cocaine abuse. *J. Neurosci.* **39**, 503–518 (2019).
56. C. A. Mejias-Aponte, C. Ye, A. Bonci, E. A. Kiyatkin, M. Morales, A subpopulation of neurochemically-identified ventral tegmental area dopamine neurons is excited by intravenous cocaine. *J. Neurosci.* **35**, 1965–1978 (2015).
57. S. Koulchitsky, B. De Backer, E. Quertemont, C. Charlier, V. Seutin, Differential effects of cocaine on dopamine neuron firing in awake and anesthetized rats. *Neuropsychopharmacology* **37**, 1559–1571 (2012).
58. M. Creed, J. Kauffling, G. R. Fois, M. Jalabert, T. Yuan, C. Lüscher, F. Georges, C. Bellone, Cocaine exposure enhances the activity of ventral tegmental area dopamine neurons via calcium-impermeable NMDARs. *J. Neurosci.* **36**, 10759–10768 (2016).
59. S. M. Fortin, M. F. Roitman, Central GLP-1 receptor activation modulates cocaine-evoked phasic dopamine signaling in the nucleus accumbens core. *Physiol. Behav.* **176**, 17–25 (2017).
60. A. M. Polter, K. Barcomb, A. C. Tsuda, J. A. Kauer, Synaptic function and plasticity in identified inhibitory inputs onto VTA dopamine neurons. *Eur. J. Neurosci.* **47**, 1208–1218 (2018).
61. A. Matsui, J. T. Williams, Opioid-sensitive GABA inputs from rostromedial tegmental nucleus synapse onto midbrain dopamine neurons. *J. Neurosci.* **31**, 17729–17735 (2011).
62. K. R. Tan, C. Yvon, M. Turiault, J. J. Mirzabekov, J. Doehner, G. Labouëbe, K. Deisseroth, K. M. Tye, C. Lüscher, GABA neurons of the VTA drive conditioned place aversion. *Neuron* **73**, 1173–1183 (2012).
63. R. van Zessen, J. L. Phillips, E. A. Budygin, G. D. Stuber, Activation of VTA GABA neurons disrupts reward consumption. *Neuron* **73**, 1184–1194 (2012).
64. M. Morales, E. B. Margolis, Ventral tegmental area: Cellular heterogeneity, connectivity and behaviour. *Nat. Rev. Neurosci.* **18**, 73–85 (2017).
65. S. R. Taylor, S. Badurek, R. J. Dileone, R. Nashmi, L. Minichiello, M. R. Picciotto, GABAergic and glutamatergic efferents of the mouse ventral tegmental area. *J. Comp. Neurol.* **522**, 3308–3334 (2014).
66. J. M. Breton, A. R. Charbit, B. J. Snyder, P. T. K. Fong, E. V. Dias, P. Himmels, H. Lock, E. B. Margolis, Relative contributions and mapping of ventral tegmental area dopamine and GABA neurons by projection target in the rat. *J. Comp. Neurol.* **527**, 916–941 (2019).
67. D. I. Brierley, M. K. Holt, A. Singh, A. de Araujo, M. McDougale, M. Vergara, M. H. Afaghani, S. J. Lee, K. Scott, C. Maske, W. Langhans, E. Krause, A. de Kloet, F. M. Gribble, F. Reimann, L. Rinaman, G. de Lartigue, S. Trapp, Central and peripheral GLP-1 systems independently suppress eating. *Nat. Metab.* **3**, 258–273 (2021).
68. S. M. Fortin, R. K. Lipsky, R. Lhamo, J. Chen, E. Kim, T. Borner, H. D. Schmidt, M. R. Hayes, GABA neurons in the nucleus tractus solitarius express GLP-1 receptors and mediate anorectic effects of liraglutide in rats. *Sci. Transl. Med.* **12**, eaay8071 (2020).
69. C. E. Geisler, L. Décarie-Spain, M. K. Loh, W. Trumbauer, J. Gaisinsky, M. E. Klug, C. Pelletier, J. F. Davis, H. D. Schmidt, M. F. Roitman, S. E. Kanoski, M. R. Hayes, Amylin modulates a ventral tegmental area-to-medial prefrontal cortex circuit to suppress food intake and impulsive food-directed behavior. *Biol. Psychiatry* **95**, 938–950 (2024).
70. A. J. Brown, D. A. Fisher, E. Kouranova, A. McCoy, K. Forbes, Y. Wu, R. Henry, D. Ji, A. Chambers, J. Warren, W. Shu, E. J. Weinstein, X. Cui, Whole-rat conditional gene knockout via genome editing. *Nat. Methods* **10**, 638–640 (2013).
71. S. M. Fortin, J. C. Chen, M. C. Petticord, F. J. Ragozzino, J. H. Peters, M. R. Hayes, The locus coeruleus contributes to the anorectic, nausea, and autonomic physiological effects of glucagon-like peptide-1. *Sci. Adv.* **9**, eadh0980 (2023).
72. Y. Zhang, M. W. Kahng, J. A. Elkind, V. R. Weir, N. S. Hernandez, L. M. Stein, H. D. Schmidt, Activation of GLP-1 receptors attenuates oxycodone taking and seeking without compromising the antinociceptive effects of oxycodone in rats. *Neuropsychopharmacology* **45**, 451–461 (2020).
73. D. J. Reiner, E. G. Miettlicki-Baase, L. E. McGrath, D. J. Zimmer, K. K. Bence, G. L. Sousa, V. R. Konanur, J. Krawczyk, D. H. Burk, S. E. Kanoski, G. E. Hermann, R. C. Rogers, M. R. Hayes, Astrocytes Regulate GLP-1 receptor-mediated effects on energy balance. *J. Neurosci.* **36**, 3531–3540 (2016).
74. C. Paxinos, G. Watson, *The Rat Brain in Stereotaxic Coordinates* (Academic Press, 1997).
75. Y. Zhang, J. Ben Nathan, A. Moreno, R. Merkel, M. W. Kahng, M. R. Hayes, B. C. Reiner, R. C. Crist, H. D. Schmidt, Calcitonin receptor signaling in nucleus accumbens D1R- and D2R-expressing medium spiny neurons bidirectionally alters opioid taking in male rats. *Neuropsychopharmacology* **48**, 1878–1888 (2023).
76. J. T. Ting, T. L. Daigle, Q. Chen, G. Feng, Acute brain slice methods for adult and aging animals: Application of targeted patch clamp analysis and optogenetics. *Methods Mol. Biol.* **1183**, 221–242 (2014).
77. B. C. Reiner, R. C. Crist, T. Borner, R. P. Doyle, M. R. Hayes, B. C. De Jonghe, Single nuclei RNA sequencing of the rat AP and NTS following GDF15 treatment. *Mol. Metab.* **56**, 101422 (2022).
78. T. Borner, C. E. Geisler, S. M. Fortin, R. Cosgrove, J. Alsina-Fernandez, M. Dogra, S. Doebley, M. J. Sanchez-Navarro, R. M. Leon, J. Gaisinsky, A. White, A. Bamezai, M. Y. Ghidewon, H. J. Grill, R. C. Crist, B. C. Reiner, M. Ai, R. J. Samms, B. C. De Jonghe, M. R. Hayes, GIP receptor agonism attenuates GLP-1 receptor agonist-induced nausea and emesis in preclinical models. *Diabetes* **70**, 2545–2553 (2021).
79. B. C. Reiner, Y. Zhang, L. M. Stein, E. D. Perea, G. Arauco-Shapiro, J. Ben Nathan, K. Ragnini, M. R. Hayes, T. N. Ferraro, W. H. Berrettini, H. D. Schmidt, R. C. Crist, Single nucleus transcriptomic analysis of rat nucleus accumbens reveals cell type-specific patterns of gene expression associated with volitional morphine intake. *Transl. Psychiatry* **12**, 374 (2022).

Acknowledgments: We thank J. B. Nathan and S. Neelamagam for technical contributions to this project. **Funding:** This work was supported in part by National Institutes of Health grants R01 DA037897 (H.D.S.), R21 DA045792 (H.D.S.), R21 DA057458 (H.D.S. and R.C.C.), and R21 DA059966 (B.C.R.). **Author contributions:** Conceptualization: R.M., N.S.H., V.W., B.C.R., and H.D.S. Methodology: R.M., N.S.H., V.W., Y.Z., B.C.R., and H.D.S. Investigation: R.M., N.S.H., V.W., Y.Z., M.T.R., A.C., R.C.C., and H.D.S. Visualization: R.M., N.S.H., R.C.C., B.C.R., and H.D.S. Software: R.M., B.C.R., R.C.C., and H.D.S. Formal analysis: R.M., N.S.H., M.T.R., R.C.C., B.C.R., and H.D.S. Supervision: N.S.H., B.C.R., and H.D.S. Project administration: R.M., N.S.H., and H.D.S. Resources: N.S.H., B.C.R., and H.D.S. Data curation: B.C.R. and H.D.S. Funding acquisition: B.C.R. and H.D.S. Validation: N.S.H., B.C.R., and H.D.S. Writing—original draft: R.M., N.S.H., V.W., and H.D.S. Writing—review and editing: R.M., N.S.H., V.W., R.C.C., B.C.R., and H.D.S. **Competing interests:** B.C.R. receives research funding from Novo Nordisk and Boehringer Ingelheim that was not used in support of these studies. B.C.R. also receives in kind support from Oxford Nanopore Technologies and 10x Genomics that was not used in support of this study. All other authors declare that they have no competing interests. **Data and material availability:** All data needed to evaluate the conclusions in the paper are present in the paper and/or the Supplementary Materials. A file containing the data point values presented in the paper is available at <https://doi.org/10.5061/dryad.djh9w0w8v>, and snRNA-seq count matrices for our discovery dataset are available at the NCBI Gene Expression Omnibus (GEO) under accession number GSE284465. The custom code used to analyze the fiber photometry data in this paper is archived at <https://zenodo.org/records/13984378>.

Submitted 3 July 2024

Accepted 28 January 2025

Published 26 February 2025

10.1126/sciadv.adr5051